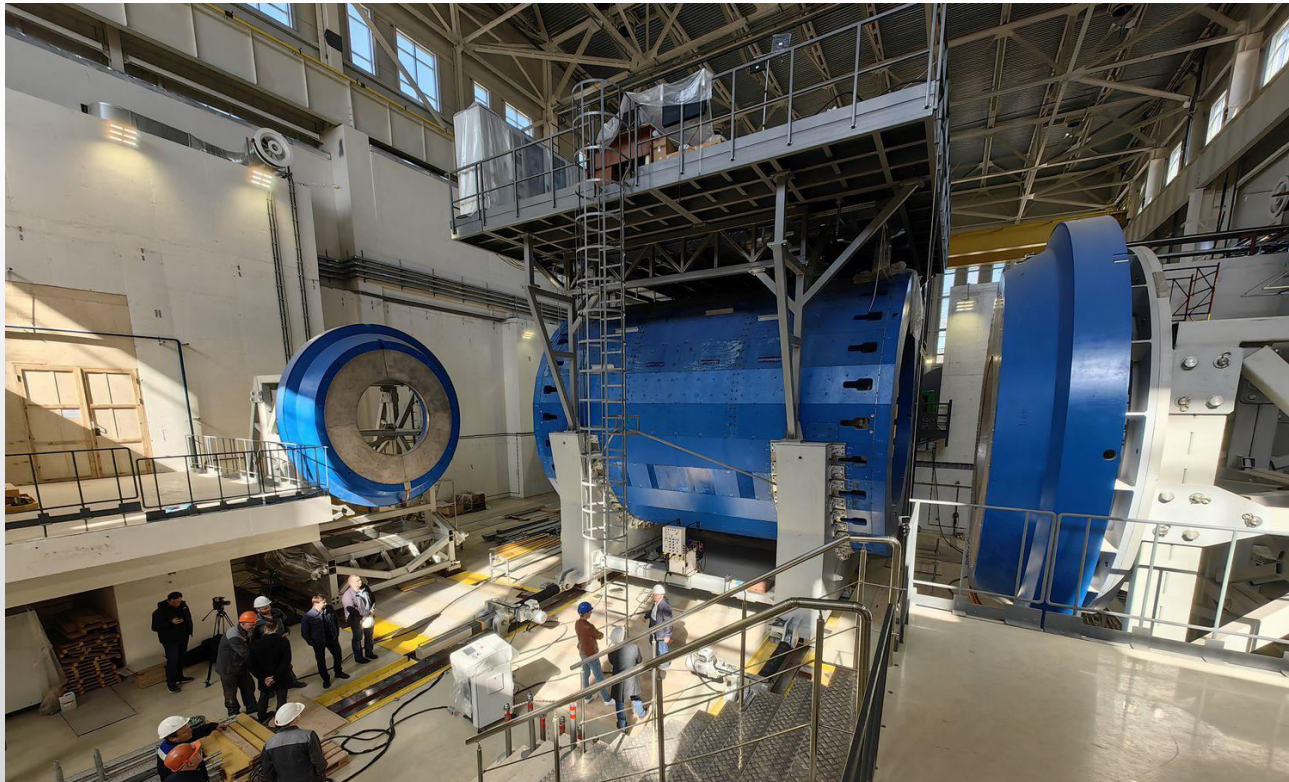




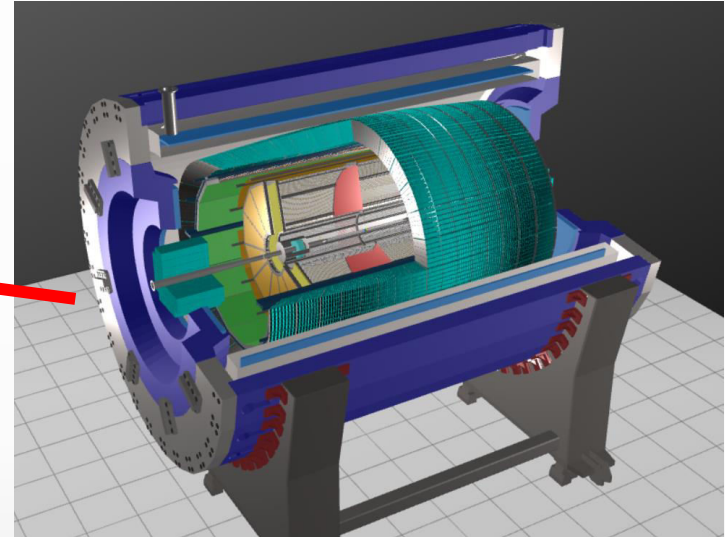
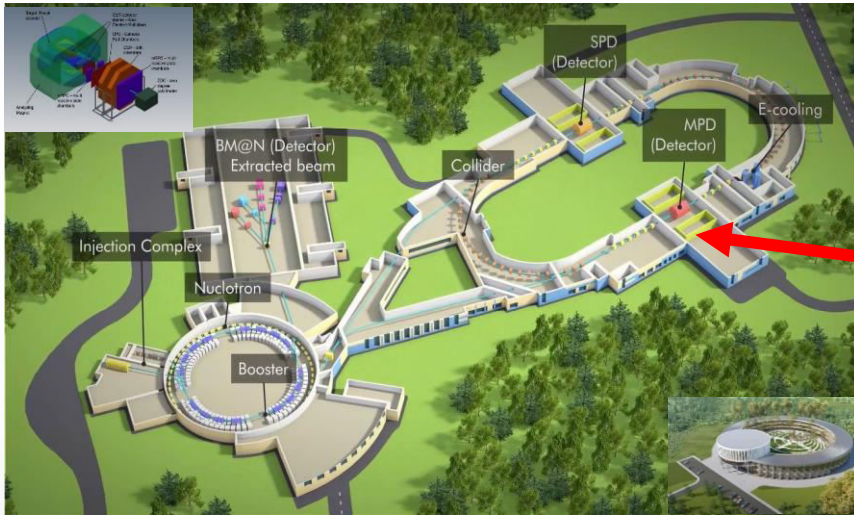
# Nuclotron based Ion Collider fAcility

## Status of the MPD experiment at NICA

V. Riabov for the MPD Collaboration



❖ One of two experiments at NICA collider to study heavy-ion collisions at  $\sqrt{s_{NN}} = 4\text{--}11$  GeV



Length	340 cm
Vessel outer radius	140 cm
Vessel inner radius	27 cm
Default magnetic field	0.5 T
Drift gas mixture	90% Ar+10% CH <sub>4</sub>
Maximum event rate	7 kHz ( $L = 10^{27}$ cm <sup>-2</sup> s <sup>-1</sup> )

❖ Expected beam condition for the first year(s) :

- ✓ not-optimal beam optics → wide z-vertex,  $\sigma_z \sim 50$  cm
- ✓ reduced luminosity ( $\sim 10^{25}$ ) → collision rate  $\sim 50$  Hz
- ✓ first beams: Bi+Bi / Xe+Xe at  $\sqrt{s_{NN}} \leq 7$  GeV

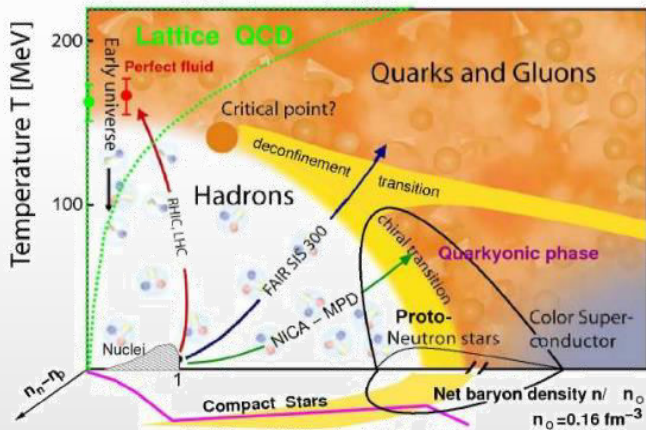
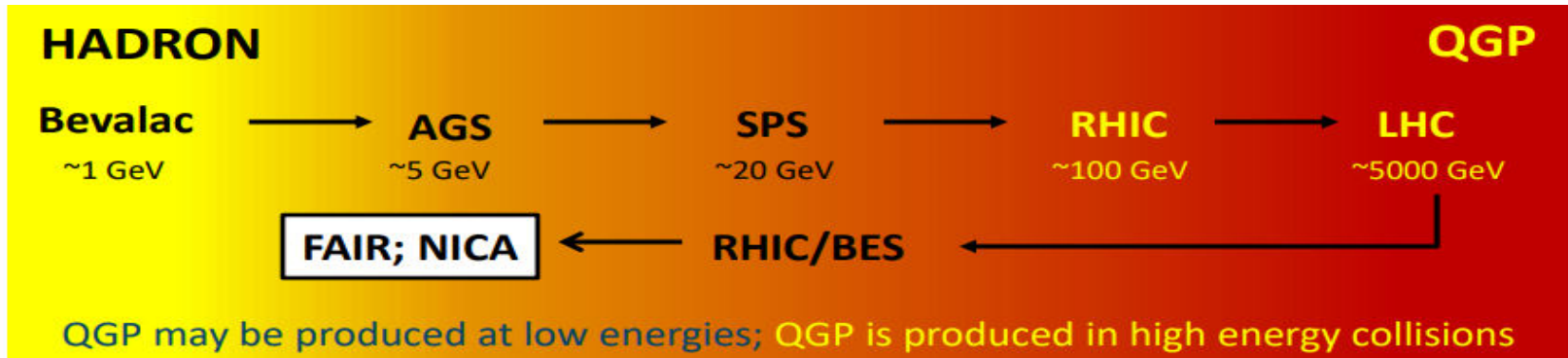
**TPC:**  $|\Delta\phi| < 2\pi$ ,  $|\eta| \leq 1.6$

**TOF, EMC:**  $|\Delta\phi| < 2\pi$ ,  $|\eta| \leq 1.4$

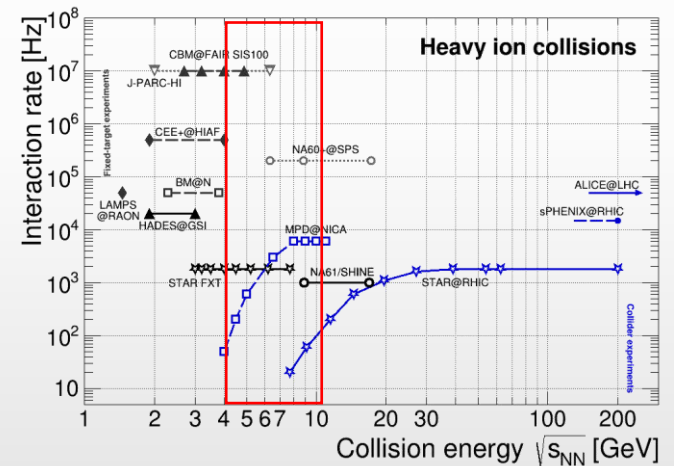
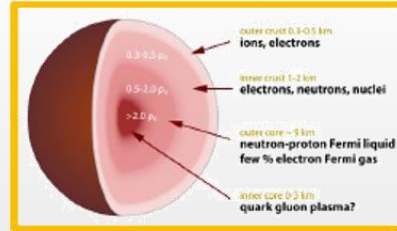
**FFD:**  $|\Delta\phi| < 2\pi$ ,  $2.9 < |\eta| < 3.3$

**FHCAL:**  $|\Delta\phi| < 2\pi$ ,  $2 < |\eta| < 5$

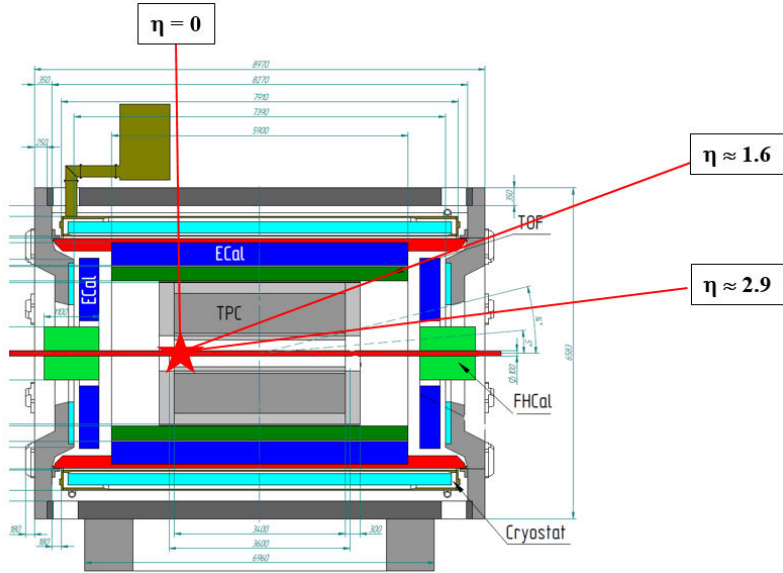
# Relativistic heavy-ion collisions



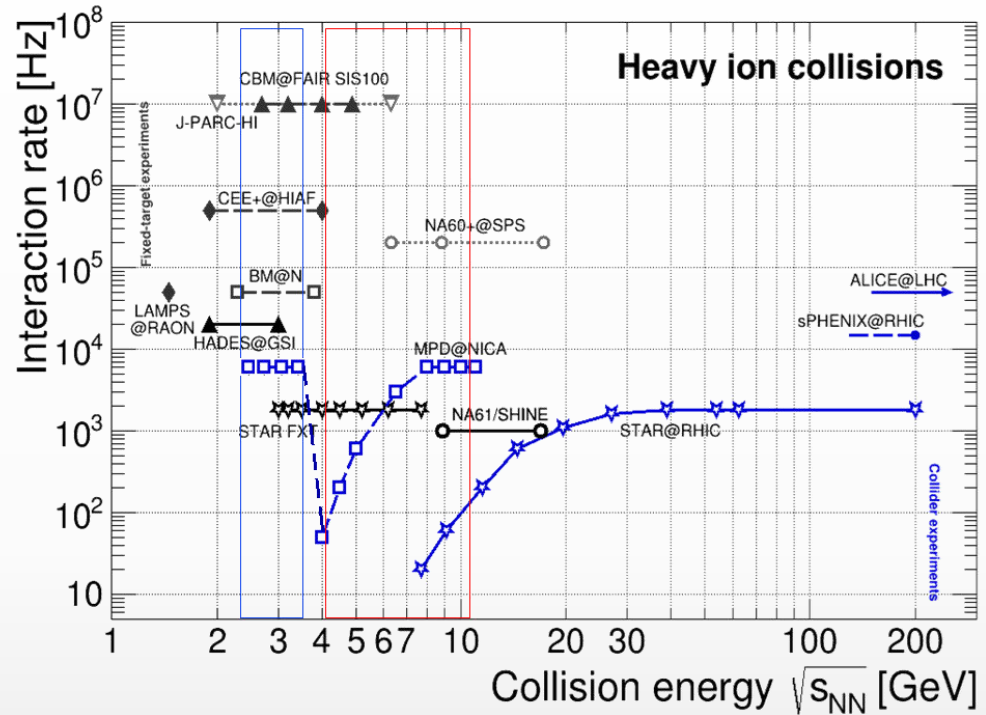
high baryon densities  
 $\rightarrow$  inner structure of compact stars



- ❖ At  $\mu_B \sim 0$ , smooth crossover (lattice QCD calculations + data)
- ❖ At large  $\mu_B$ , 1<sup>st</sup> order phase transition is expected  $\rightarrow$  QCD critical point
- ❖ MPD will study QCD medium at extreme net baryon densities
- ❖ Many ongoing (NA61/Shine, STAR-BES) and future experiments (CBM) in  $\sim$  same energy range



Ebeam	$\sqrt{s_{NN}}$ collider mode	$\sqrt{s_{NN}}$ FXT mode	$\eta_{CM}$	CMS coverage
2.0	4	2.4	0.7	-0.7; 0.9 (2.2)
5.5	11	3.5	1.23	-1.23; 0.37 (1.67)

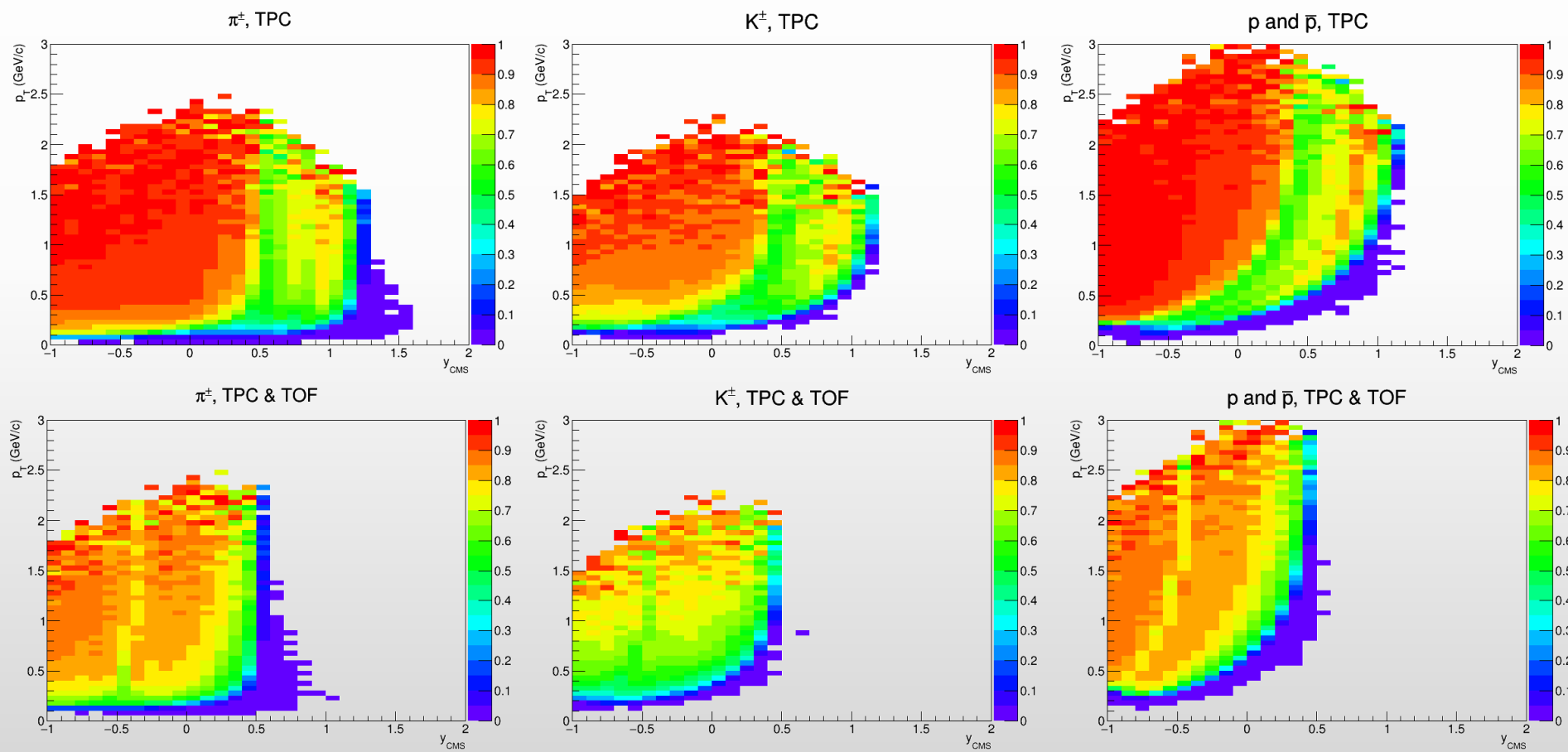


- ❖ Fixed-target mode: one beam + thin wire ( $\sim 100 \mu\text{m}$ ) close to the edge of the MPD central barrel:
  - ✓ extends energy range of MPD to  $\sqrt{s_{NN}} = 2.4\text{-}3.5 \text{ GeV}$  (overlap with HADES, BM@N and CBM)
  - ✓ solves problem of low event rate at lower collision energies (only  $\sim 50 \text{ Hz}$  at  $\sqrt{s_{NN}} = 4 \text{ GeV}$  at design luminosity)
  - ✓ backup start-up solution (too low luminosity, only one beam, etc.)

# Detector performance in FXT mode

- ❖ Existing trigger system (FFD + FHCAL + TOF) remains to be efficient in the fixed-target mode
- ❖ MPD detector provides reasonable midrapidity coverage for identified hadrons
- ❖ Reconstruction efficiencies for TPC and TPC+TOF charged tracks at maximum beam energy:

Basic track selections:  $N_{\text{hits}} > 10$ ;  $\text{DCA-to-PV} < 2$  cm; primary particles



MPD detector is able to run in the fixed-target mode in the default configuration

- ❖ MPD strategy – high-luminosity scans in energy and system size to measure a wide variety of signals:
  - ✓ order of the phase transition and search for the QCD critical point → structure of the QCD phase diagram
  - ✓ hypernuclei and equation of state at high baryon densities → inner structure of compact stars, star mergers
  
- ❖ Scans to be carried out using the same apparatus with all the advantages of collider experiments:
  - ✓ maximum phase space, minimally biased acceptance, free of target parasitic effects
  - ✓ correlated systematic effects for different systems and energies → simplified extraction of physical signals
  
- ❖ Continuously develop physical program based on the recent advancements in the field:
  - ✓ identified particle spectra and ratios, collective flow and femtoscopy, production of strangeness and hypernuclei net-proton fluctuations, global polarization of hyperon and spin alignment of vector mesons, dilepton continuum and LVMs, etc.

# Activities in the MPD Hall

Top platform (cryogenics, power supplies, control system)



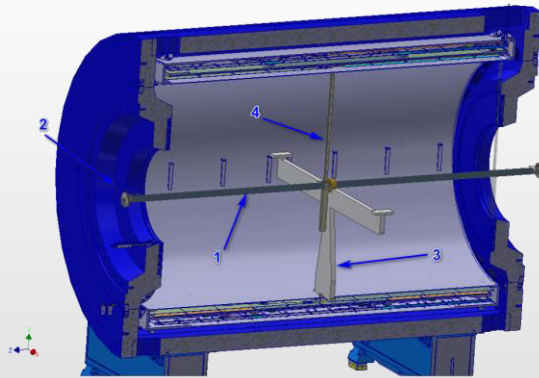
Chimney



Cryogenic platform



Novosibirsk BINP magnetic field mapper



1. Aluminum (carbon fiber plastic) guiding rod
2. End cap fixation
3. Intermediate support
4. Carbon fiber plastic carriage

Parameter	Value
Length of movement for Z	2 × 4,5 m
Length of movement for R	0,1 – 2,2 m
Rotation of measurement block	3600
Accuracy of movement for Z	50 microns
Accuracy of movement for R	50 microns
Accuracy of rotation	0,20
Hall 3D sensor	HE444, HE Hoeben Electronix,
Hall 3D sensor accuracy	0,1 Gs
Hall 3D sensor accuracy total (with accuracy of laser tracker and temperature correction)	0,3 Gs
Sag of guide line	5 mm
Weight of mapper	100 kg
Reading time per one measurement	1 sec

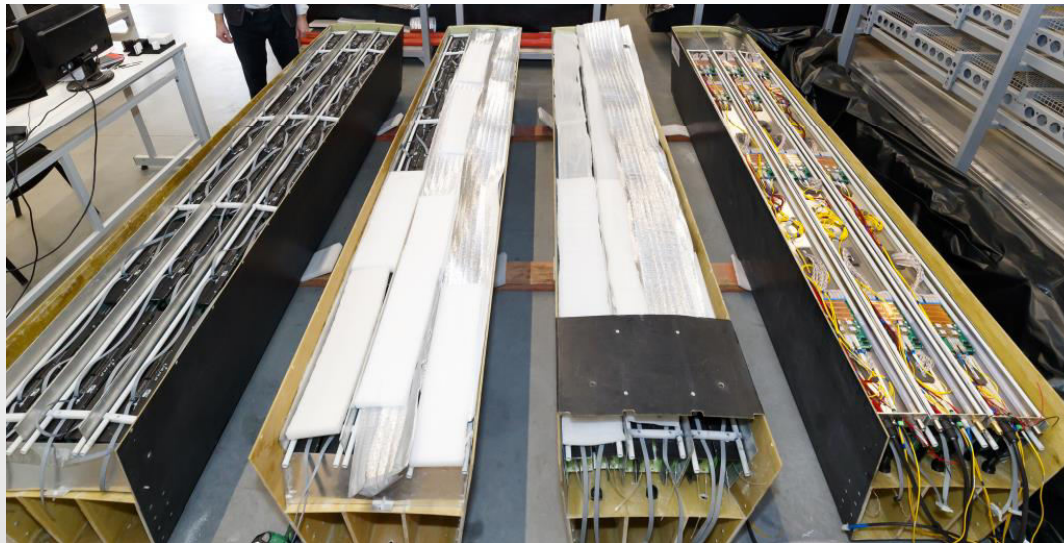
Carbon fiber support frame sagita ~ 5 mm at full load



- ❖ Yoke, TRIM coils, top platform, chimney assembled, ongoing tests of the refrigerators and control Dewar
- ❖ Cooling to LN2 and LHe temperatures by the end of 2023 → MF measurements → central support frame

- ❖ Sampling calorimeter with projective geometry (~70 tons):
  - ✓ 25 sectors (50 half-sectors); 2400 modules; 38,400 “shashlyk”-type Pb-Sc towers with segmentation of 4x4 cm<sup>2</sup>
- ❖ 1600 modules (66%) have been produced (800 in Russia + 800 in China)
- ❖ Production of additional 400 modules in Russia is ongoing, use Russian-made WLS fibers → 83% in total
- ❖ Mass production of half-sectors in JINR by international team, 18 half-sectors assembled

Half-sectors at different stages of assembly



ECAL installation in the MPD: August, 2024



- ❖ The production of MRPC detectors was completed in September 2022, (107%) chambers
- ❖ TOF modules are assembled → long-term cosmic ray tests
- ❖ Electronics & cables, HV distribution modules, installation equipment - in stock
- ❖ Assembly of the TOF gas system in the MPD hall → spring, 2023

Storage of tested TOF modules



TOF installation bench in LHEP



- ❖ The equipment for installing the modules in the MPD is ready for use and stored in the laboratory

TOF installation in the MPD: September, 2024

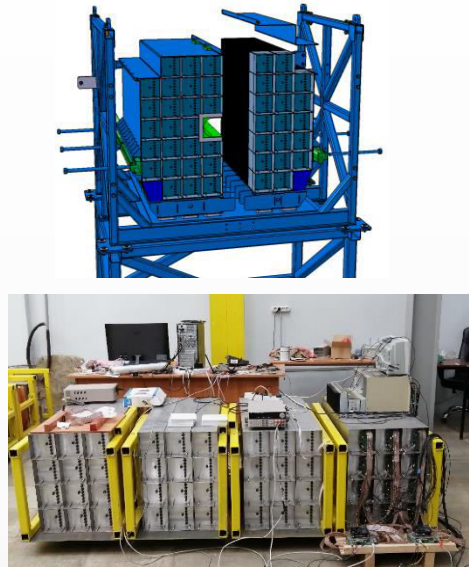
- ❖ TPC cylinders, central membrane and service wheels are ready, final vessel assembly by the end of 2023
- ❖ Read-out chambers (ROCs) - 24 tested chambers in stock + 4 tested spare chambers



- ❖ Gas system ready – testing
- ❖ TPC FE electronics status:
  - ✓ 65% manufactured (967 pc)
  - ✓ no more problems with components → 100% available
- ❖ On critical path:
  - ✓ TPC rails prod./inst. – October-November, 2023
  - ✓ TPC cooling system – (INP BSU, Belarus):  
FEE cooling ready by Spring, 2024;  
thermostabilization panels by September, 2024;

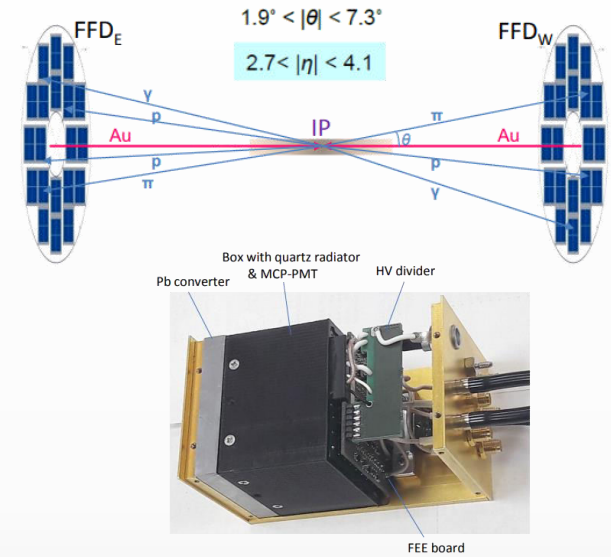
TPC installation in the MPD: end of 2024

## FHCAL



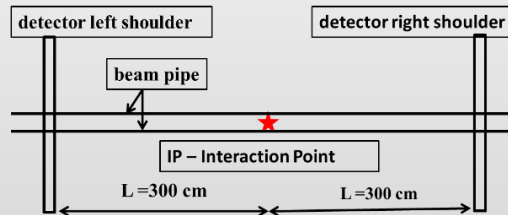
FHCAL modules have been produced and tested → installation in autumn 2023

## FFD



Cherenkov modules of FFDE and FFDW are available, mechanics of FFD sub-detectors is available for installation in container with vacuum beam tube

## Beam and luminosity monitoring



Measurement of transverse sizes of the bunches  
 Transvers and longitudinal convergence of bunches  
 Vertices distribution along the beam

- ❖ Two sets by 32 scintillator counters readout by SIMPs from both sides
- ❖ Observables & methods:
  - ✓ counting rate and z-vertex distribution ( $\sigma_{z\text{-vertex}} \sim 5\text{ cm}$  with  $\delta\tau \sim 300\text{ ps}$ )
  - ✓ Van der Meer and  $\Delta Z$  scans for optimization of beam optics
- ❖ Beam tests of prototypes
- ❖ Mass production of scintillator detectors

- ❖ Trigger system consists of FFD ( $2.7 < |\eta| < 4.1$ ), FHCAL ( $2 < |\eta| < 5$ ) and TOF ( $|\eta| < 1.5$ )

- ❖ MPD trigger system challenges at NICA energies:

- ✓ low multiplicity of particles produced in heavy-ion collisions
- ✓ particles are not ultra-relativistic (even the spectator protons)

- ❖ DCM-QGSM-SMM, BiBi@9.2: trigger efficiency is 87-98% for different trigger configuration

- FFD trigger definition:

- ✓ at least one fired module per side
- ✓ meaningful times,  $0 < \text{time}_{E,W} < 50 \text{ ns}$
- ✓ reconstructed z-vertex,  $|z\text{-vertex}| < 140 \text{ cm}$

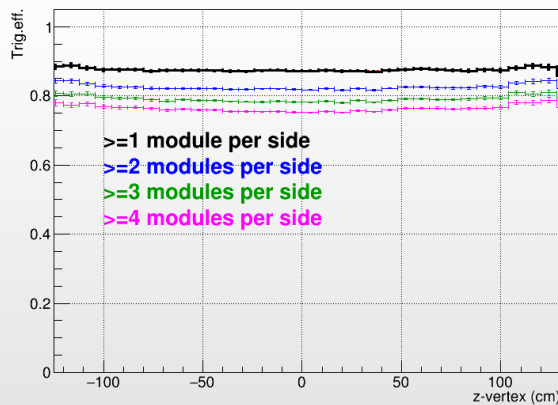
- FHCAL trigger definition:

- ✓ at least one fired module per side
- ✓ meaningful times,  $0 < \text{time}_{E,W} < 50 \text{ ns}$
- ✓ reconstructed z-vertex,  $|z\text{-vertex}| < 150 \text{ cm}$

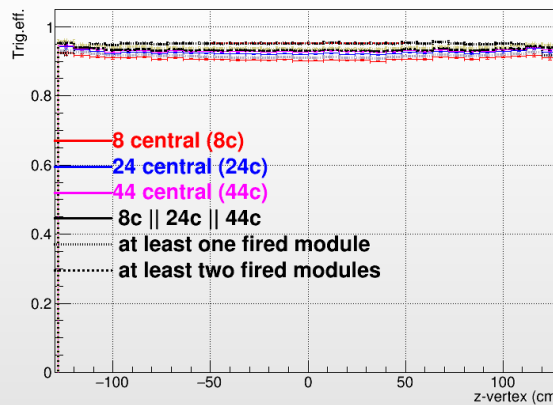
- TOF trigger definition:

- ✓ at least one fired MRPC

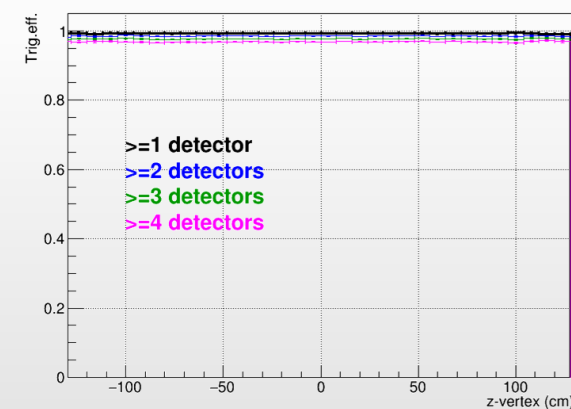
FFD trigger efficiency vs. z-vertex



FHCAL trigger efficiency vs. z-vertex



TOF trigger efficiency vs. z-vertex

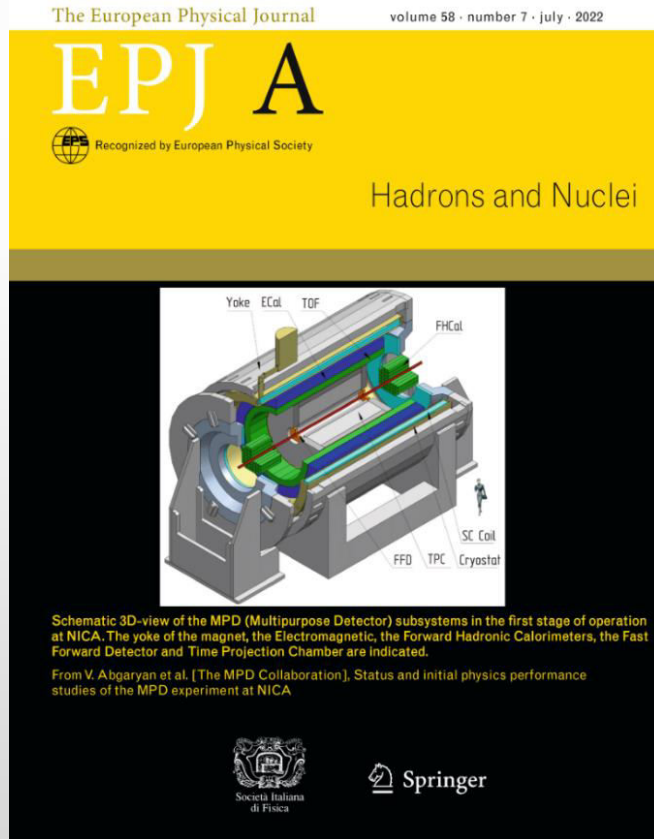


- ❖ Trigger system of the MPD based on FFD, FHCAL and TOF detectors provides high efficiency in HIC

- ❖ Light collision systems:  $\sim 50\%$  for C+C, vanishingly small for d+d

- ❖ MPD publications: over 200 in total for hardware, software and physics studies (SPIRES)
- ❖ MPD @ conferences: presented at all major conferences in the field
- ❖ First collaboration paper recently published EPJA (~ 50 pages): Eur.Phys.J.A 58 (2022) 7, 140

## Status and initial physics performance studies of the MPD experiment at NICA



Eur. Phys. J. A manuscript No.  
(will be inserted by the editor)

### Status and initial physics performance studies of the MPD experiment at NICA

The MPD Collaboration<sup>1</sup>  
<sup>1</sup>The full list of Collaboration Members is provided at the end of the manuscript

Received: April 20, 2022 / Accepted: date

Abstract: The Nuclotron-based Ion Collider Facility (NICA) is under construction at the Joint Institute for Nuclear Research (JINR), with commissioning of the facility expected in late 2022. The Multi-Purpose Detector (MPD) has been designed to operate at NICA and its components are currently in production. The detector is expected to be ready for data taking with the first beams from NICA. This document provides an overview of the landscape of the investigation of the QCD phase diagram in the region of maximum baryon density, where NICA and MPD will be able to provide significant and unique input. It also provides a detailed description of the MPD set-up, including its various subsystems as well as its support and computing infrastructures. Selected performance studies for particular physics measurements at MPD are presented and discussed in the context of existing data and theoretical expectations.	<ul style="list-style-type: none"> <li>1.1 The Inner Tracking System . . . . . 22</li> <li>1.2 The Particle Detector . . . . . 23</li> <li>1.3 The Cosmic Ray Detector . . . . . 23</li> <li>1.4 Infrastructure and support systems . . . . . 24</li> <li>1.5 MPD Hall . . . . . 25</li> <li>1.5.1 Mechanical, installation, and support structure . . . . . 25</li> <li>1.5.2 Support systems . . . . . 26</li> <li>1.5.3 Electronics . . . . . 26</li> <li>1.5.4 Slow Control System . . . . . 26</li> <li>1.5.5 Data Acquisition . . . . . 26</li> <li>2 Software development and computing resources for the MPD experiment . . . . . 27</li> <li>2.1 Software . . . . . 27</li> <li>2.2 Computing . . . . . 27</li> <li>2.3 Preparation for data taking . . . . . 28</li> <li>3 Description of physics feasibility studies . . . . . 28</li> <li>3.1 Centrality determination . . . . . 29</li> <li>3.2 Bulk properties: hadron spectra, yields and ratios . . . . . 31</li> <li>3.3 Particle reconstruction . . . . . 33</li> <li>3.3.1 <math>d, A</math> and <math>z</math> reconstruction . . . . . 33</li> <li>3.3.2 <math>u, s</math> and <math>J/\psi</math> reconstruction . . . . . 33</li> <li>3.4 Reconstruction of resonances . . . . . 35</li> <li>3.5 Electromagnetic probe . . . . . 37</li> <li>3.6 Anisotropic flow . . . . . 40</li> <li>3.7 Event-by-event hadron and net-charge fluctuations . . . . . 42</li> <li>4 Conclusions . . . . . 43</li> <li>A Appendix . . . . . 50</li> </ul>
---	---

**Contents**

1 Introduction . . . . . 1	1
1.1 Brief survey of the MPD physics goal . . . . . 4	4
1.2 Hadronometry . . . . . 4	4
1.3 Anisotropic flow measurements . . . . . 5	5
1.4 Intensity interferometry . . . . . 7	7
1.5 Resonance . . . . . 7	7
1.6 Short-lived resonances . . . . . 8	8
1.7 Electromagnetic probe . . . . . 10	10
2 MPD apparatus . . . . . 11	11
2.1 Magnet . . . . . 12	12
2.2 Time Projection Chamber . . . . . 13	13
2.3 Fast Forward Detector . . . . . 15	15
2.4 Electromagnetic Calorimeter . . . . . 16	16
2.5 Forward Hadronic Calorimeter . . . . . 17	17
2.6 Fast Forward Detector . . . . . 21	21
2.7 Plans for additional detectors . . . . . 21	21

**1 Introduction**

The Multi-Purpose Detector (MPD) is one of the two dedicated heavy-ion collision experiments at the Nuclotron-based Ion Collider Facility (NICA), one of the flagship projects, planned to come into operation at the Joint Institute for Nuclear Research (JINR) in 2022. Its main scientific purpose is to search for novel phenomena in the baryon-rich region of the QCD phase diagram by means of colliding heavy nuclei in the energy range of  $4 \text{ GeV} \leq \sqrt{s_{NN}} \leq 11 \text{ GeV}$ .

**G. Feofilov, A. Aparin**

## Global observables

- Total event multiplicity
- Total event energy
- Centrality determination
- Total cross-section measurement
- Event plane measurement at all rapidities
- Spectator measurement

**V. Kolesnikov, Xianglei Zhu**

## Spectra of light flavor and hypernuclei

- Light flavor spectra
- Hyperons and hypernuclei
- Total particle yields and yield ratios
- Kinematic and chemical properties of the event
- Mapping QCD Phase Diag.

**K. Mikhailov, A. Taranenko**

## Correlations and Fluctuations

- Collective flow for hadrons
- Vorticity,  $\Lambda$  polarization
- E-by-E fluctuation of multiplicity, momentum and conserved quantities
- Femtoscopy
- Forward-Backward corr.
- Jet-like correlations

**D. Peresunko, Chi Yang**

## Electromagnetic probes

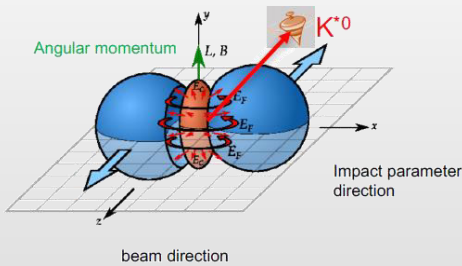
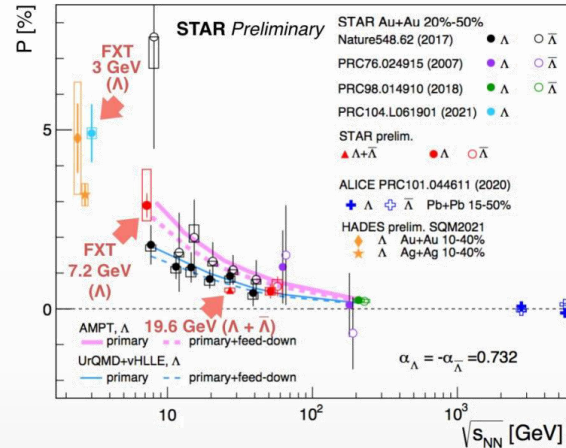
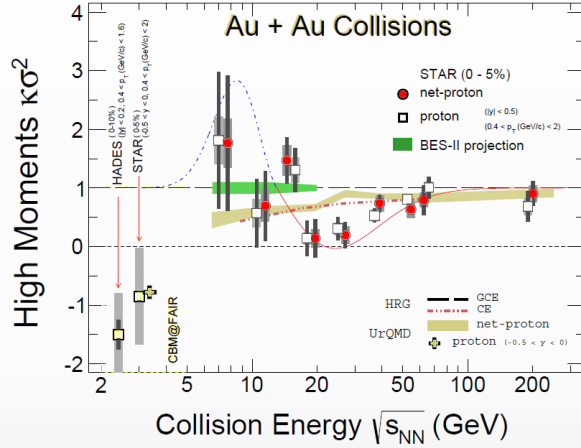
- Electromagnetic calorimeter meas.
- Photons in ECAL and central barrel
- Low mass dilepton spectra in-medium modification of resonances and intermediate mass region

**Wangmei Zha, A. Zinchenko**

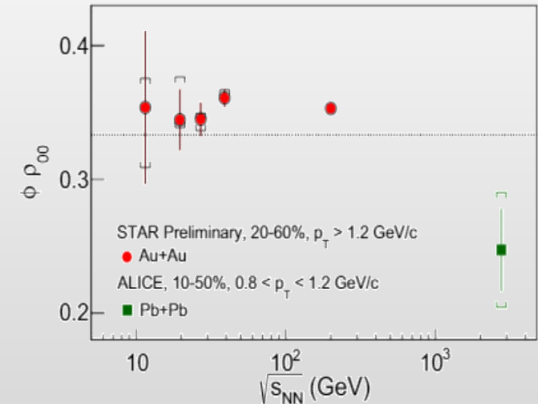
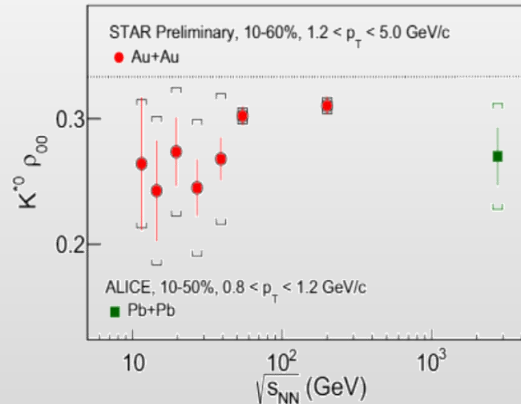
## Heavy flavor

- Study of open charm production
- Charmonium with ECAL and central barrel
- Charmed meson through secondary vertices in ITS and HF electrons
- Explore production at charm threshold

- ❖ Critical fluctuations for (net)proton/kaon multiplicity distributions
- ❖ Global hyperon polarization in mid-central A+A collisions ( $\Lambda$ ,  $\Xi$ ,  $\Omega$  and antiparticles)
- ❖ Spin alignment of vector mesons ( $K^*(892)$ ,  $\phi(1020)$ )



$$\frac{dN}{d\cos\theta} = N_0 [1 - \rho_{0,0} + \cos^2\theta (3\rho_{0,0} - 1)]$$

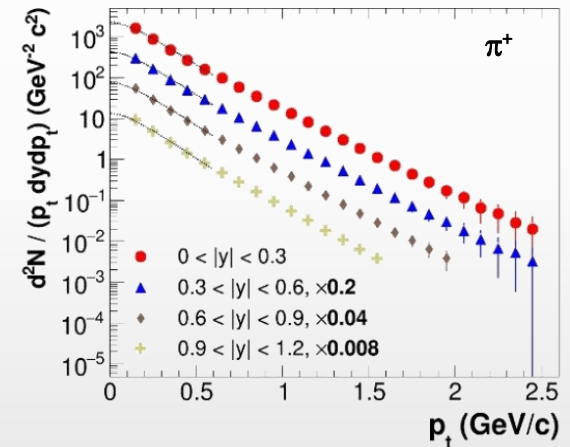
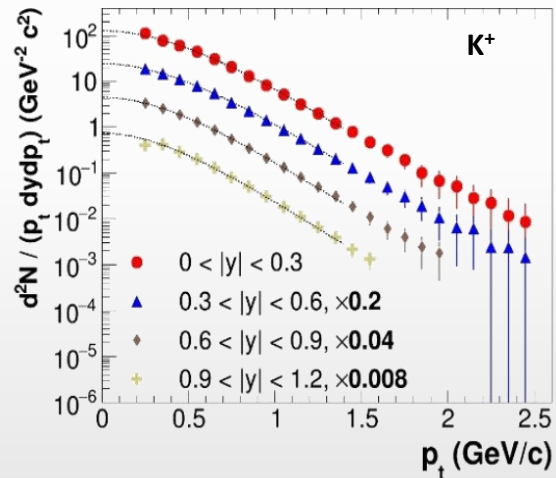
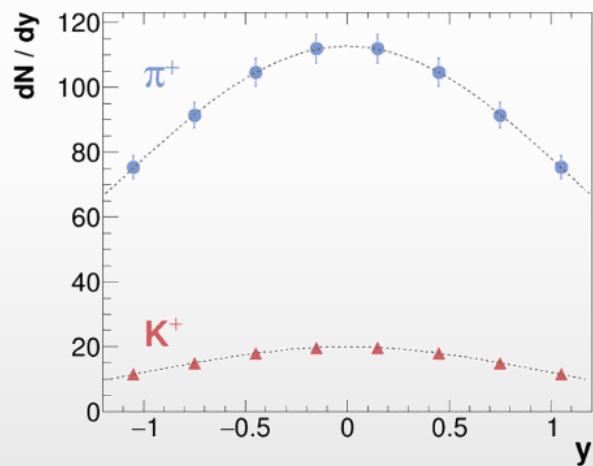


Task for the MPD: extra points in the energy range 4-11 GeV with small uncertainties

- ❖ Probe freeze-out conditions, collective expansion, hadronization mechanisms, strangeness production (“horn” for  $K/\pi$ ), parton energy loss, etc. with particles of different masses, quark contents/counts
- ❖ Charged hadrons: large and uniform acceptance + excellent PID capabilities of TPC and TOF

0-5% central AuAu@9 GeV (PHSD), 5 M events  $\rightarrow$  full event/detector simulation and reconstruction

*Phys.Part.Nucl. 53 (2022) 2, 203-206*

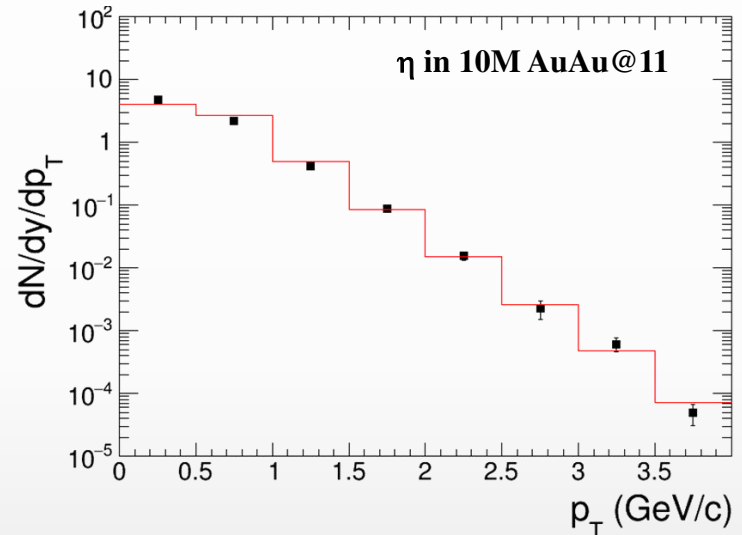
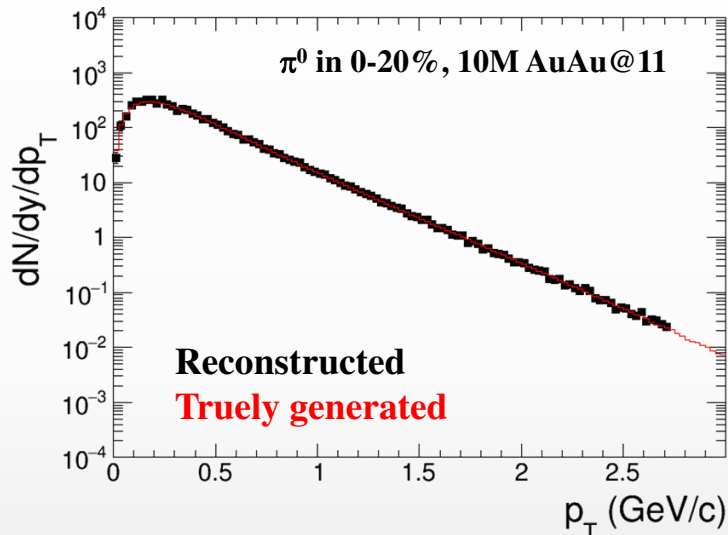


- ✓ sample  $\sim 70\%$  of the  $\pi/K/p$  production in the full phase space
- ✓ hadron spectra are measured from  $p_T \sim 0.1$  GeV/c



- ❖ Neutral mesons ( $\pi^0$ ,  $\eta$ ,  $K_s$ ,  $\omega$ ,  $\eta'$ ): ECAL reconstruction + photon conversion method (PCM)

AuAu@11 GeV (UrQMD), 10M events  $\rightarrow$  full event/detector simulation and reconstruction



- ✓ extend  $p_T$  ranges of charged particle measurements
- ✓ different systematics

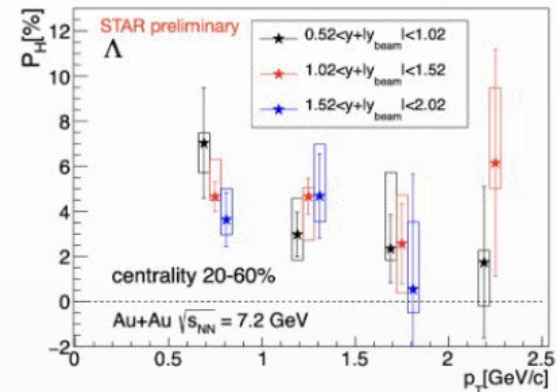
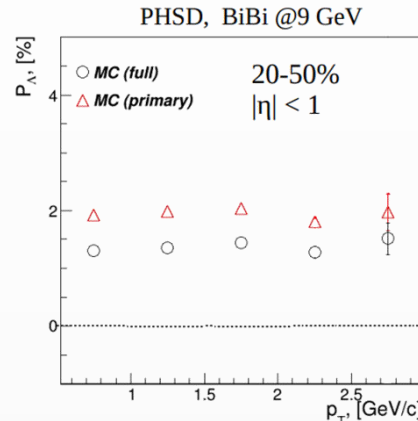
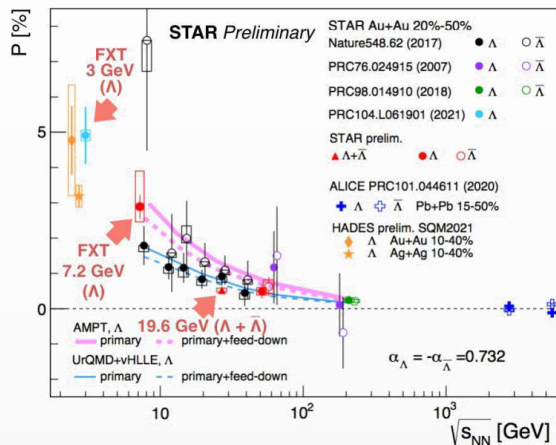
MPD will be able to measure differential production spectra, integrated yields and  $\langle p_T \rangle$ , particle ratios, multiplicity distributions for a wide variety of identified hadrons ( $\pi$ ,  $K$ ,  $\eta$ ,  $\omega$ ,  $p$ ,  $\eta'$ )

First measurements will be possible with the first sampled data sets

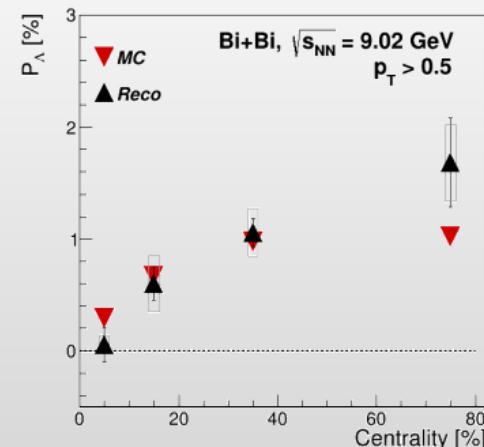
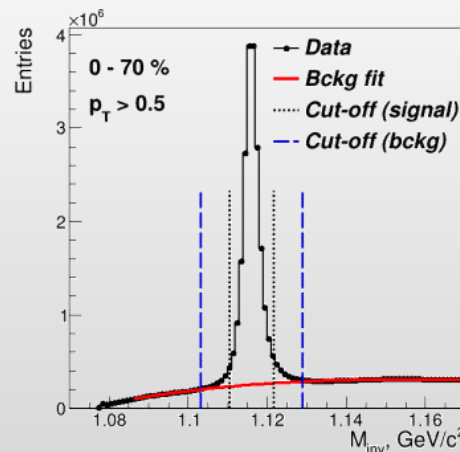
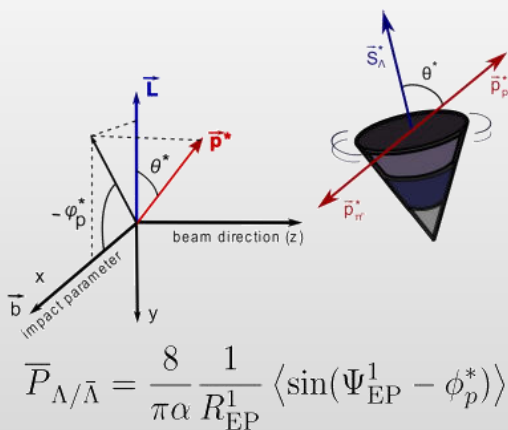
# Hyperon global polarization

- ❖ BiBi@9.2 GeV (PHSD), 15 M events → full event/detector simulation and reconstruction
- ❖ Global hyperon polarization (thermodynamical Becattini approach [1]) by the event generator → reproduce at generator level basic features measured by STAR

[1] F. Becattini, V. Chandra, L. Del Zanna

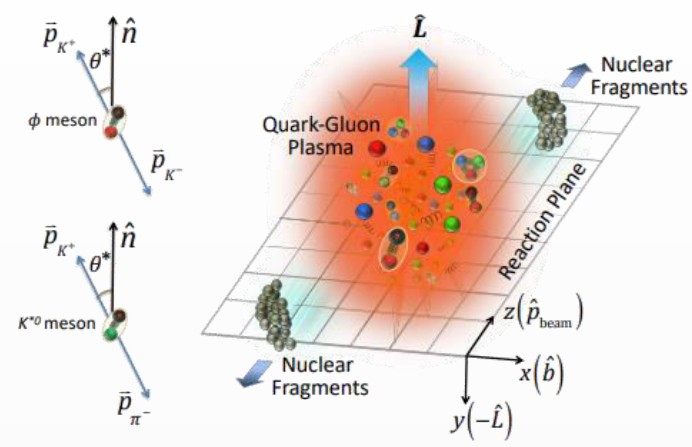


- ❖ Reconstruction of  $\Lambda$  global polarization, BiBi@9.2 GeV:



First global polarization measurements for  $\Lambda/\bar{\Lambda}$  will be possible with  $\sim 10M$  data sampled events

Non-central heavy-ion collisions:



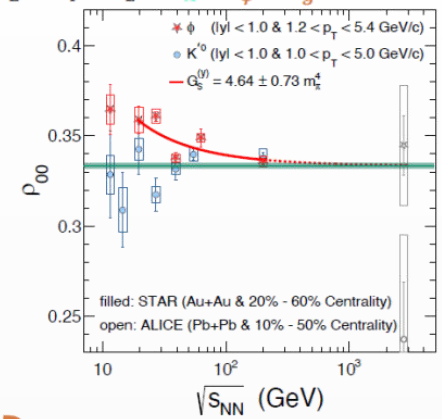
$$\frac{dN}{d\cos\theta} = N_0 [1 - \rho_{0,0} + \cos^2\theta (3\rho_{0,0} - 1)]$$

$\rho_{0,0}$  is a probability for vector meson to be in spin state = 0  $\rightarrow \rho_{0,0} = 1/3$  corresponds to no spin alignment

## The large $\rho_{00}$ puzzle

$$\rho_{00} \approx \frac{1}{3} + C_\Lambda + C_\varepsilon + C_E + C_F + C_L + C_A + C_\phi + C_g$$

Physics Mechanisms	( $\rho_{00}$ )
$c_\Lambda$ : Quark coalescence vorticity & magnetic field <sup>[1]</sup>	$< 1/3$ (Negative $\sim 10^{-5}$ )
$c_\varepsilon$ : E-comp. of Vorticity tensor <sup>[1]</sup>	$< 1/3$ (Negative $\sim 10^{-4}$ )
$c_E$ : Electric field <sup>[2]</sup>	$> 1/3$ (Positive $\sim 10^{-5}$ )
$c_F$ : Fragmentation <sup>[3]</sup>	$> \text{or}, < 1/3$ ( $\sim 10^{-5}$ )
$c_L$ : Local spin alignments <sup>[4]</sup>	$< 1/3$
$c_A$ : Turbulent color field <sup>[5]</sup>	$< 1/3$
$c_\phi$ : Vector meson strong force field <sup>[6]</sup>	$> 1/3$ (Can accommodate large positive signal)
$c_g$ : Glasma fields + effective potential	could be significant



STAR, Nature 614 244 (2023)  
 Nature 614 244 (2023)  
**strong force**

$\phi$  exhibits surprisingly large global spin alignment while  $K^*$  displays little.

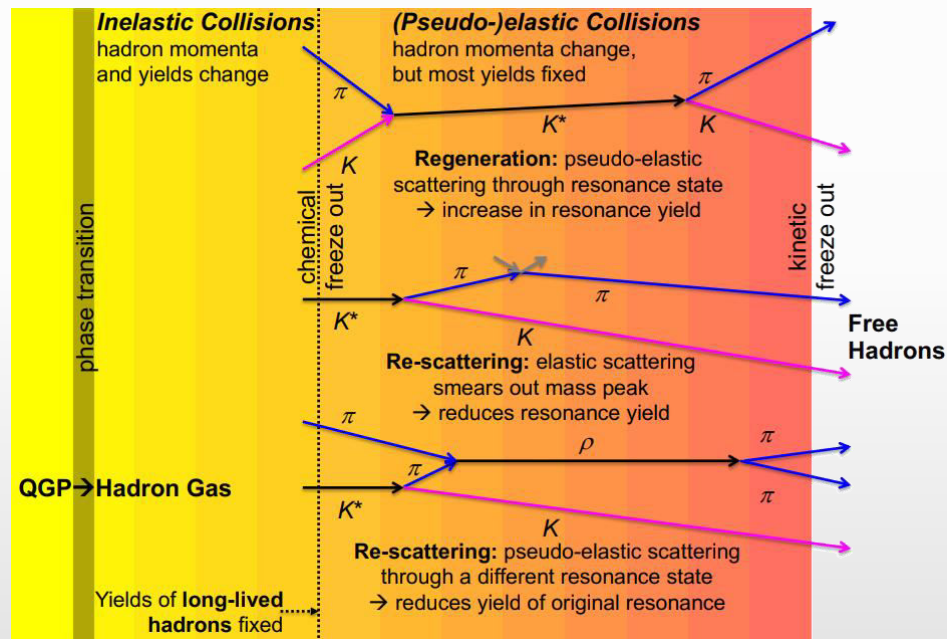
- ❖ Measurements at RHIC/LHC challenge theoretical understanding  $\rightarrow \rho_{00}$  can depend on multiple physics mechanisms (vorticity, magnetic field, hadronization scenarios, lifetimes and masses of the particles ...)
- ❖ Measurements should be extended to lower collision energies

# Hadronic phase

- ❖ Resonances probe reaction dynamics and particle production mechanisms vs. system size and  $\sqrt{s_{NN}}$ :
  - ✓ hadron chemistry and strangeness production, lifetime and properties of the hadronic phase, etc.

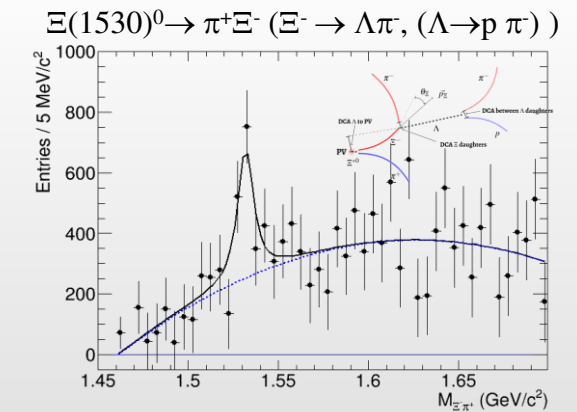
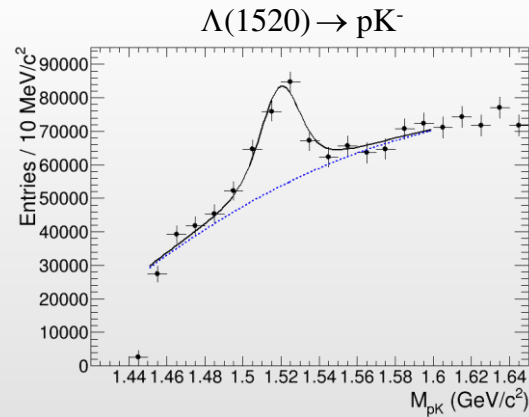
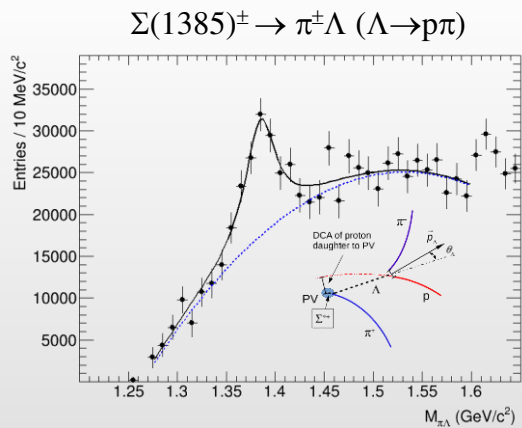
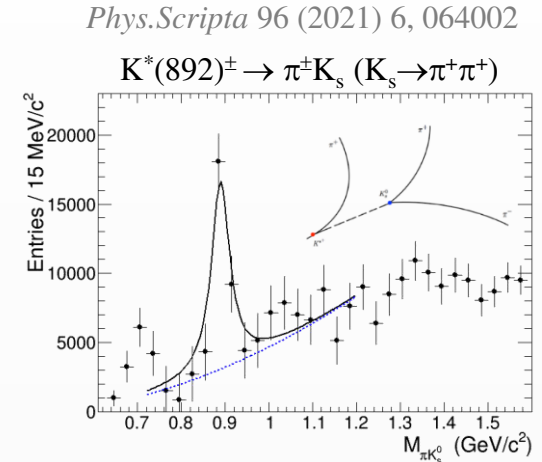
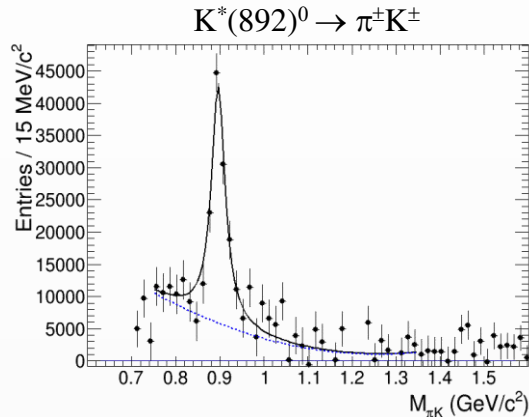
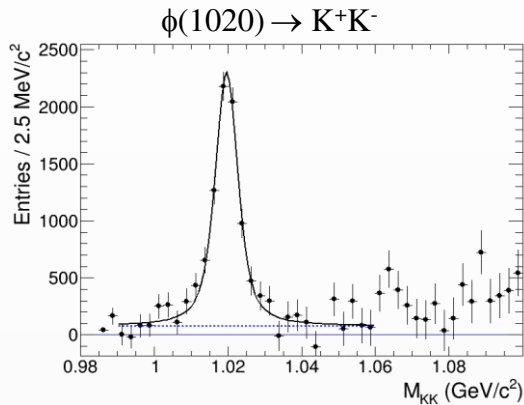
increasing lifetime  $\longrightarrow$

	$\rho(770)$	$K^*(892)$	$\Sigma(1385)$	$\Lambda(1520)$	$\Xi(1530)$	$\phi(1020)$
$c\tau$ (fm/c)	1.3	4.2	5.5	12.7	21.7	46.2
$\sigma_{\text{rescatt}}$	$\sigma_{\pi}\sigma_{\pi}$	$\sigma_{\pi}\sigma_K$	$\sigma_{\pi}\sigma_{\Lambda}$	$\sigma_K\sigma_p$	$\sigma_{\pi}\sigma_{\Xi}$	$\sigma_K\sigma_K$



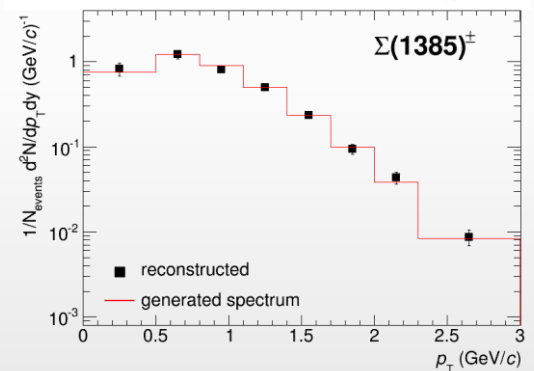
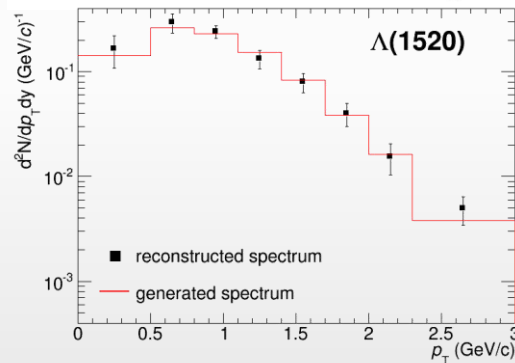
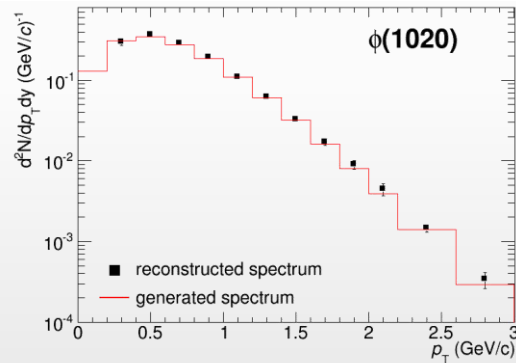
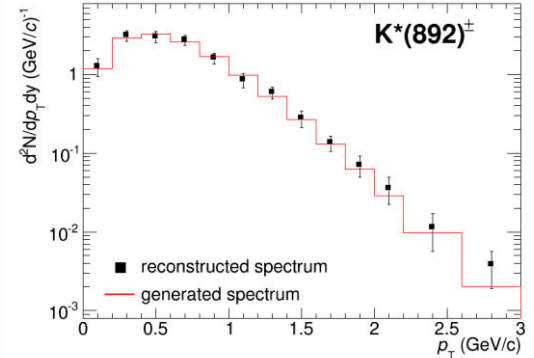
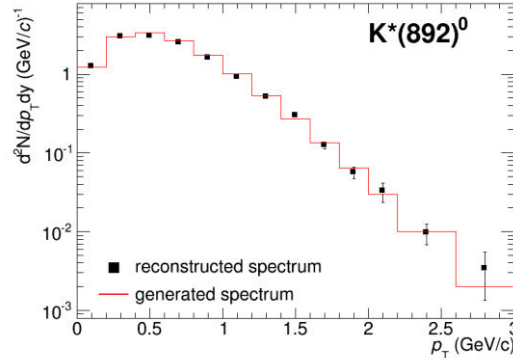
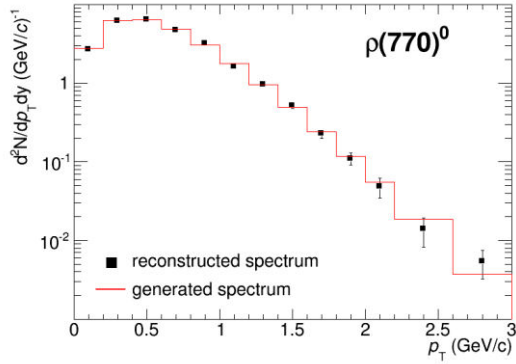
- ❖ Final state yields of resonances depend on:
  - ✓ resonance yields at chemical freeze-out
  - ✓ lifetime of the resonance and the hadronic phase
  - ✓ type and scattering cross sections of daughter particles

- ❖ BiBi@9.2 GeV (UrQMD) after mixed-event background subtraction, 10M events
- ❖ Examples of the low- $p_T$  bins



- ❖ MPD is capable of reconstruction the resonance peaks in the invariant mass distributions using combined charged hadron identification in the TPC and TOF
- ❖ Weakly decaying daughters require additional second vertex and topology cuts for reconstruction

- ❖ Full chain simulation and reconstruction,  $p_T$  ranges are limited by the possibility to extract signals,  $|y| < 1$

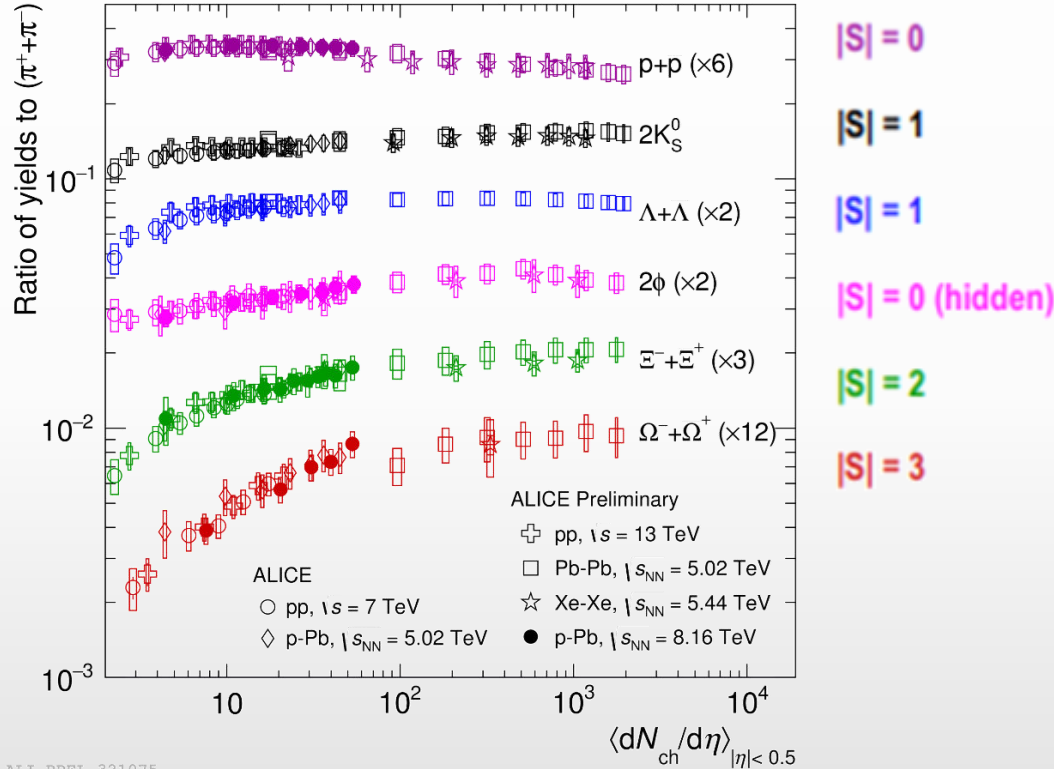


- ❖ Reconstructed spectra match the generated ones within uncertainties
- ❖ First measurements for resonances will become possible with accumulation of  $\sim 10^7$  Bi+Bi events
- ❖ Measurements are possible starting from  $\sim$  zero momentum  $\rightarrow$  sample most of the yields
- ❖ Measurements of  $\Xi(1530)^0$  are very statistics hungry

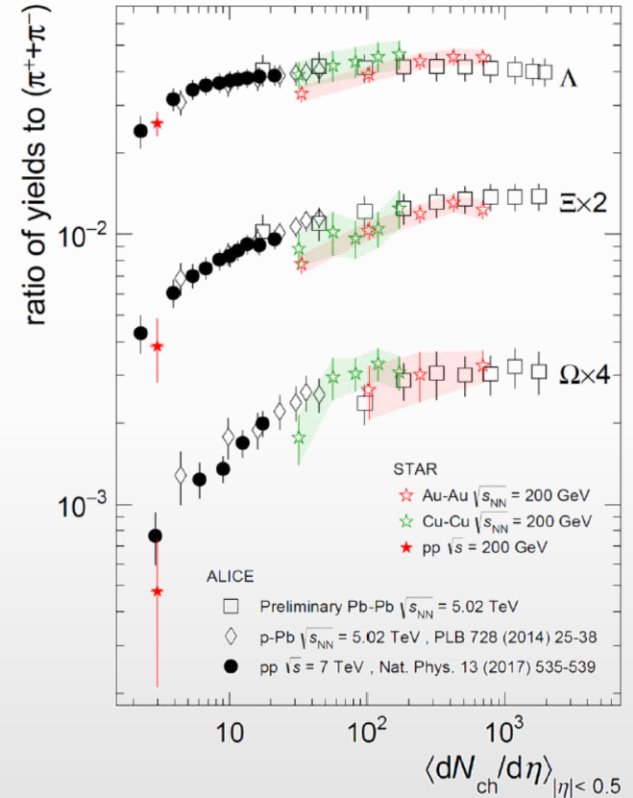
# Strangeness production: pp, p-A, A-A

- ❖ Since the mid 80s, strangeness enhancement is considered as a signature of the QGP formation
- ❖ Experimentally observed in heavy-ion collisions at AGS, SPS, RHIC and LHC energies

*Nature Phys.* 13 (2017) 535



ALI-PREL-321075

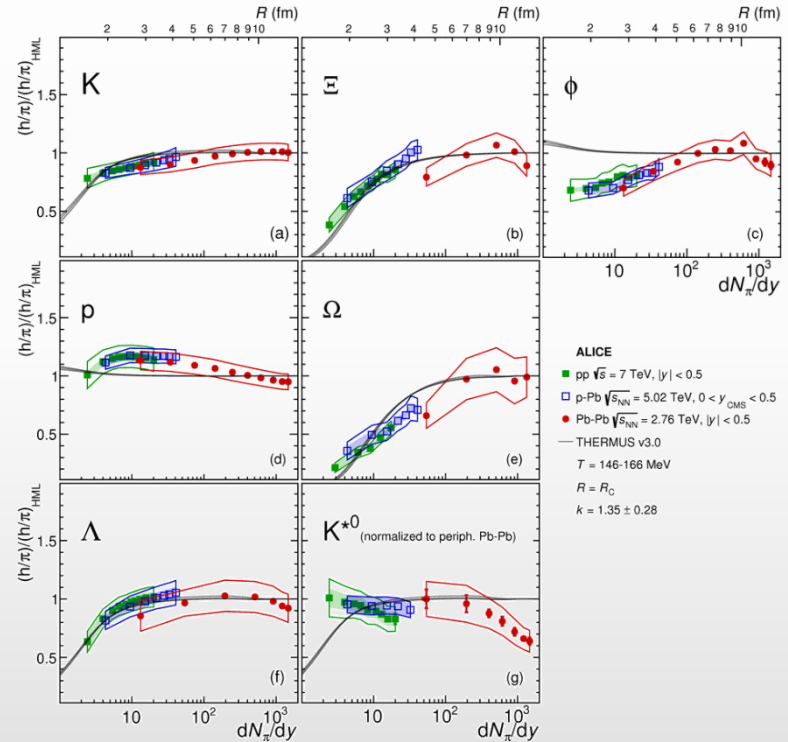
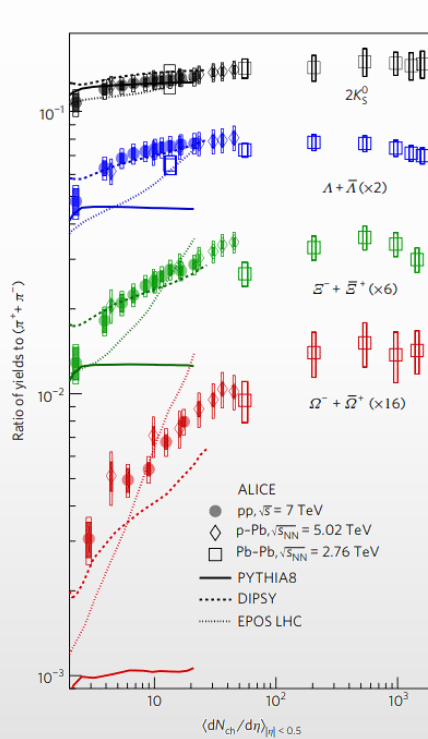


- ❖ Smooth evolution vs. multiplicity in pp, p-A and A-A collisions at LHC energies
- ❖ Strangeness enhancement increases with strangeness content and particle multiplicity
- ❖ STAR @ RHIC measurements in pp, A-A are in agreement with ALICE @ LHC at similar  $\langle dN_{ch}/d\eta \rangle$

- ❖ Origin of the strangeness enhancement in small/large systems is under debate:
  - ✓ strangeness enhancement in QGP contradicts with the observed collision energy dependence
  - ✓ strangeness suppression in pp within canonical suppression models reproduces most of results except for  $\phi(1020)$

*Nature Physics volume 13, pages535–539 (2017)*

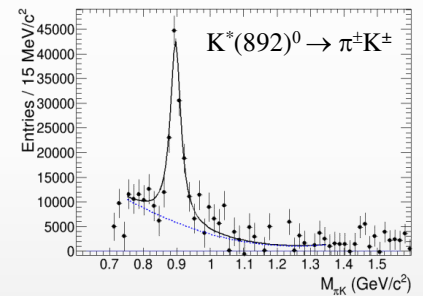
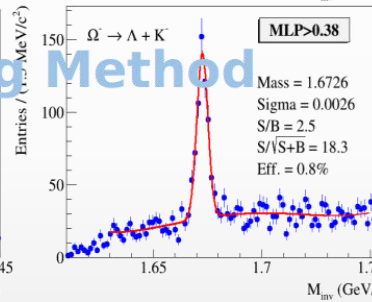
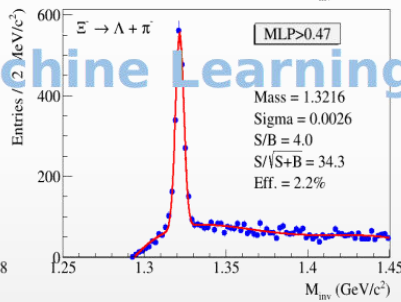
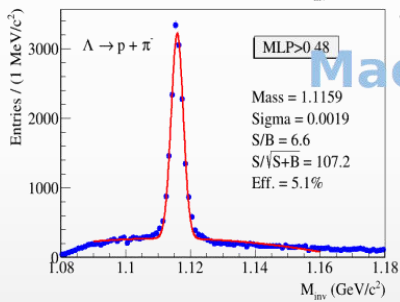
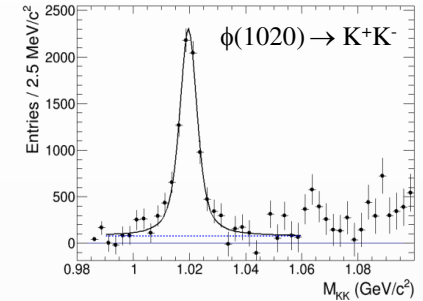
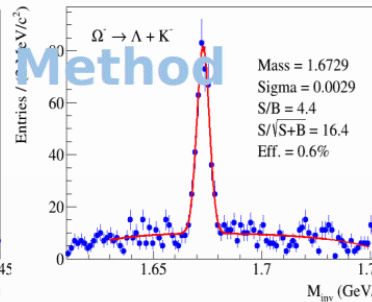
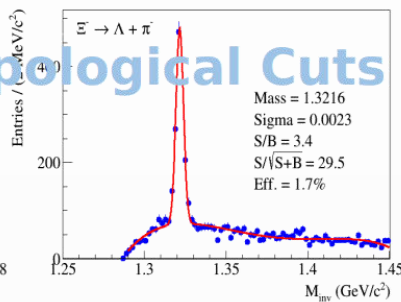
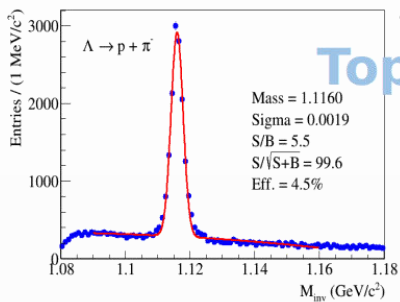
*V. Vislavicius, A. Kalweit, arXiv:1610.03001*



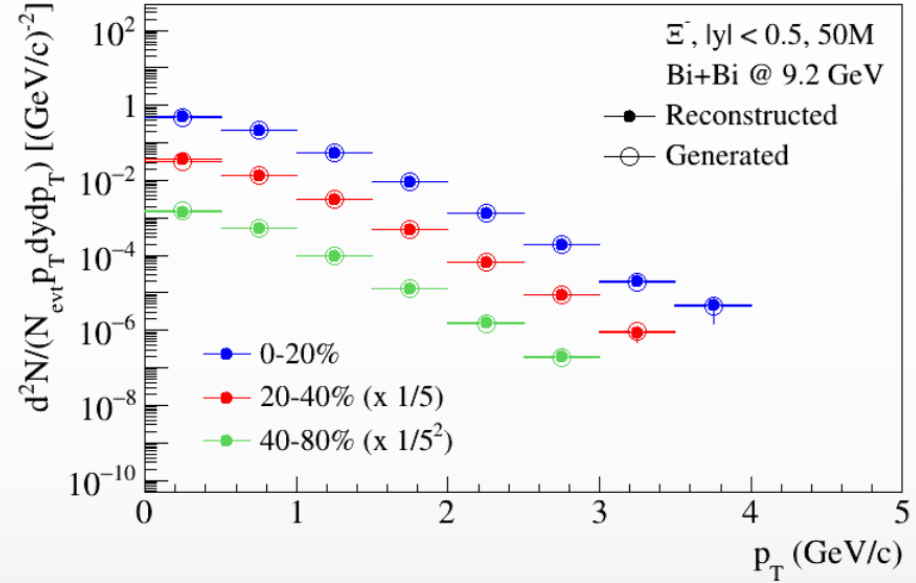
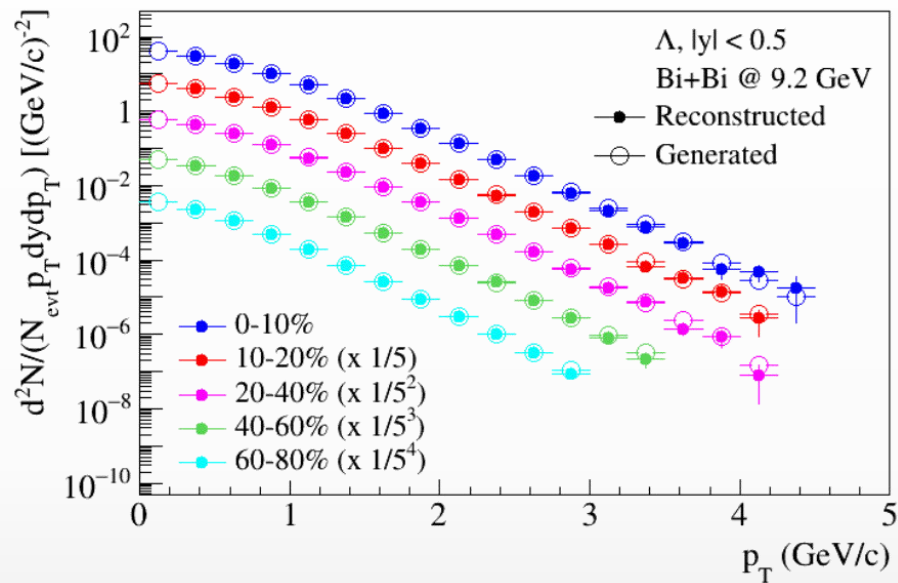
- ❖ System size scan is important



BiBi@9.2 GeV (UrQMD), 10 M events



Phys.Scripta 96 (2021) 6, 064002

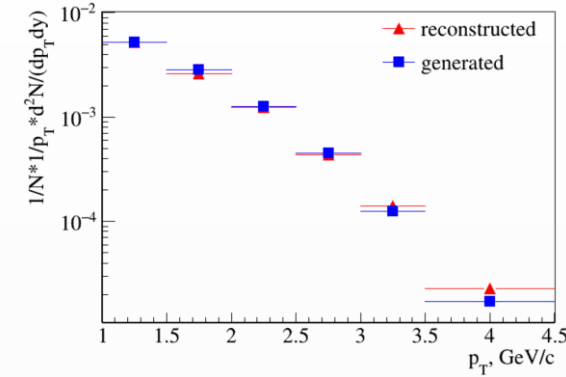
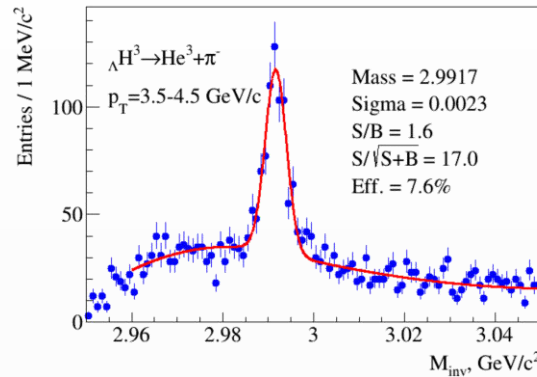
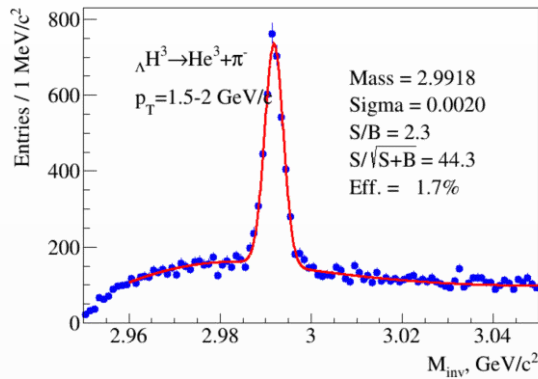


- ❖ Capability to reconstruct baryon yields down to low momenta with reasonable efficiencies
- ❖ High- $p_T$  reach is limited by statistics
- ❖ Reconstructed spectra are consistent with the generated ones  $\rightarrow$  validation of the procedure

MPD has capabilities to measure production of strange kaons, (multi)strange baryons and resonances in pp, p-A and A-A collisions using charged hadron identification in the TPC&TOF and different decay topology selections

BiBi@9.2 GeV (PHQMD), 40 M events → full event/detector simulation and reconstruction

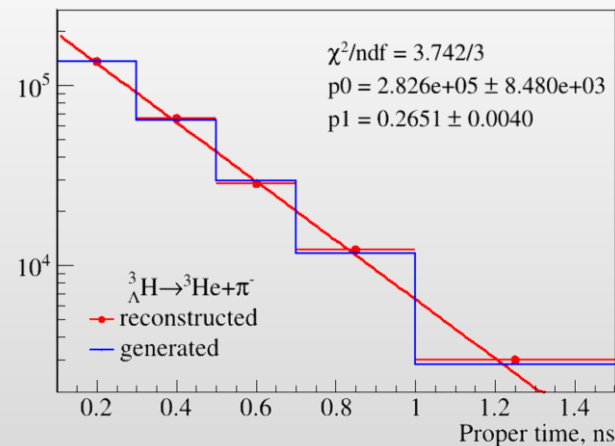
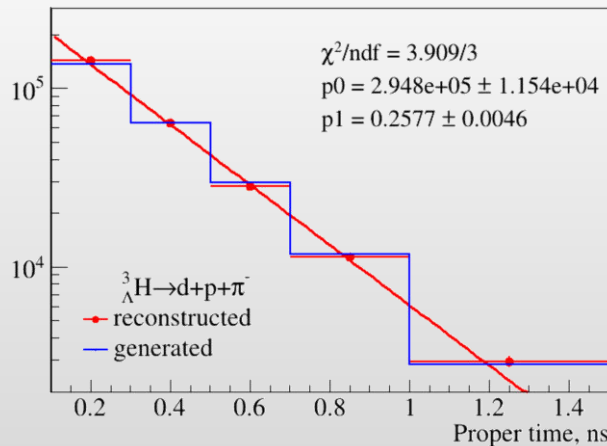
*Phys.Part.Nucl.Lett. 19 (2022) 1, 46-53*



2- and 3-prong decay modes were studied separately to estimate systematics

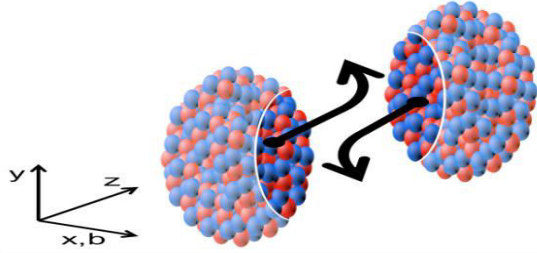
$$N(\tau) = N(0) \exp\left(-\frac{\tau}{\tau_0}\right) = N(0) \exp\left(-\frac{ML}{cp\tau_0}\right),$$

Decay channel	Branching ratio	Decay channel	Branching ratio
$\pi^- + {}^3\text{He}$	24.7%	$\pi^- + p + p + n$	1.5%
$\pi^0 + {}^3\text{H}$	12.4%	$\pi^0 + n + n + p$	0.8%
$\pi^- + p + d$	36.7%	$d + n$	0.2%
$\pi^0 + n + d$	18.4%	$p + n + n$	1.5%



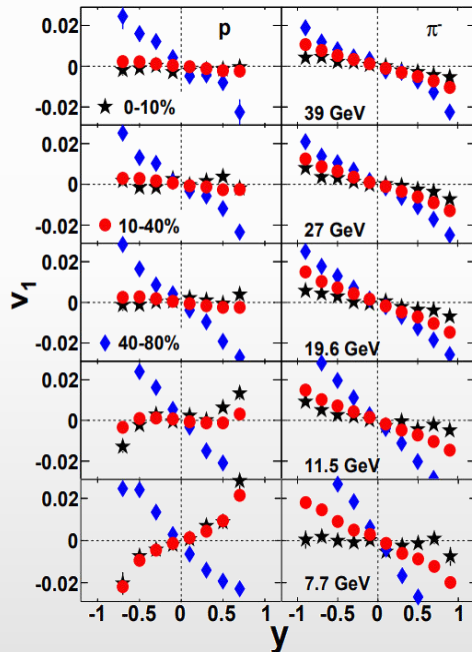
- ❖ First measurements for hypertriton will be possible with accumulation of ~ 50 M BiBi@9.2 events
- ❖ Measurements for heavier  ${}^4_\Lambda\text{H} \rightarrow {}^4\text{He} + \pi^-$  and  ${}^4_\Lambda\text{He} \rightarrow {}^3\text{He} + p + \pi^-$  would require ~ 150M events

# Beam energy dependence



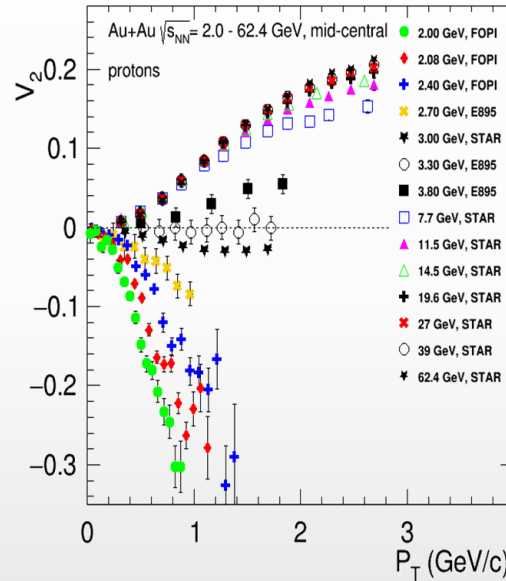
- ❖ Generated during the nuclear passage time  $(2R/\gamma)$  – sensitive to EOS
- ❖ RHIC @ 200 GeV  $(2R/\gamma) \sim 0.1$  fm/c
- ❖ AGS @ 3-4.5 GeV  $(2R/\gamma) \sim 9-5$  fm/c
- ❖  $v_1$  and  $v_2$  show strong centrality, energy and species dependence

*Phys.Rev.Lett. 112 (2014) 16, 162301*

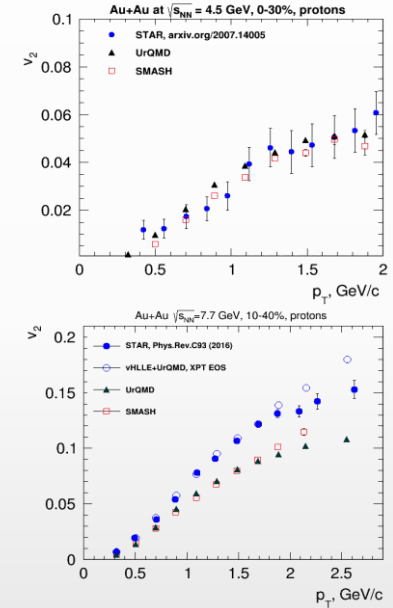


✓ models do not reproduce measurements

*EPJ Web Conf. 204 (2019) 03009*



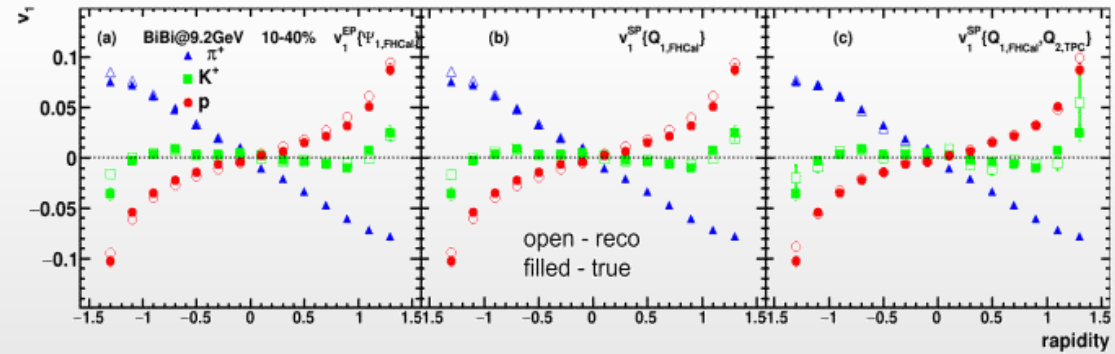
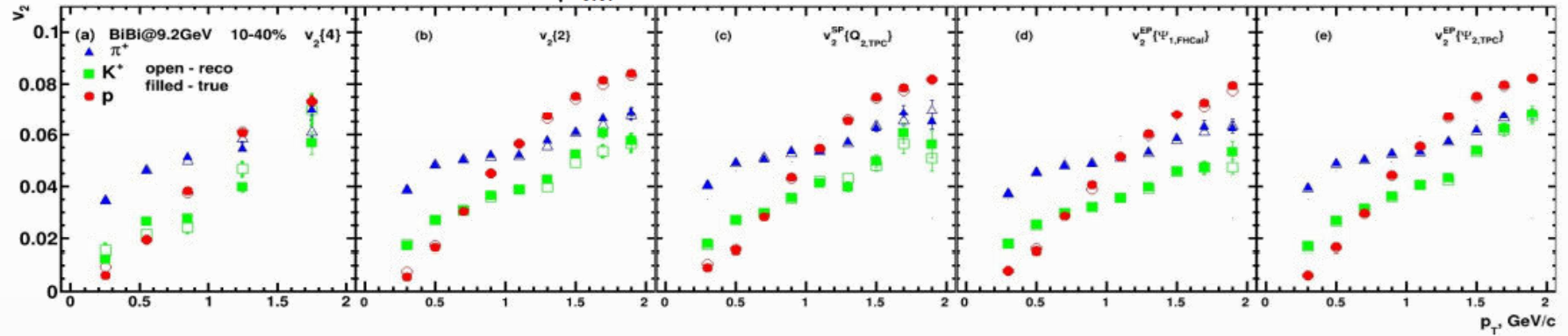
- ✓  $\sqrt{s_{NN}} \sim 3-4.5$  GeV, pure hadronic models reproduce  $v_2$  (JAM, UrQMD)  $\rightarrow$  degrees of freedom are the interacting baryons
- ✓  $\sqrt{s_{NN}} \geq 7.7$  GeV, need hybrid models with QGP phase (vHLLE+UrQMD, AMPT with string melting,...)



System size scan for flow measurements is vital for understanding of the medium transport properties and onset of the phase transition  $\rightarrow$  unique capability of the MPD in the NICA energy range

❖ UrQMD, BiBi@9.2 GeV

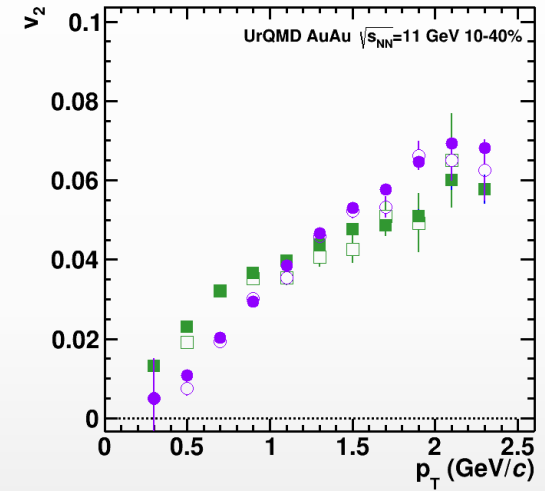
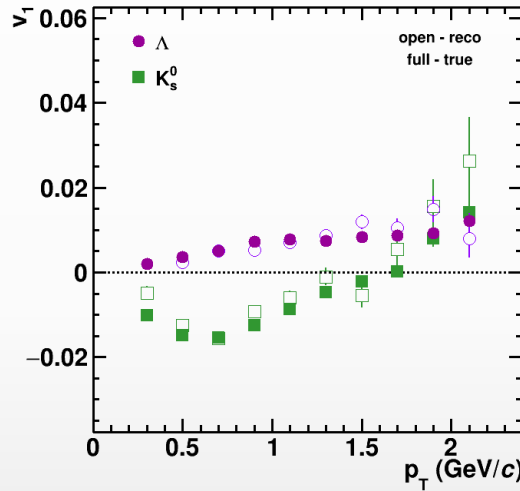
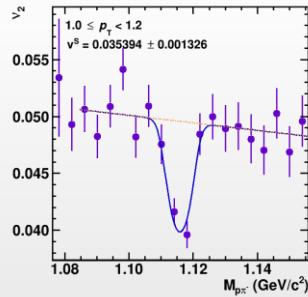
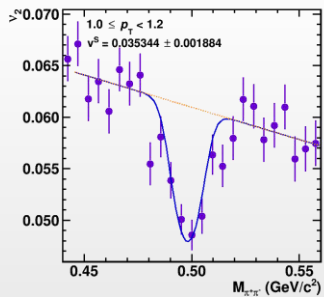
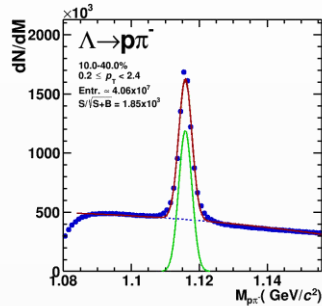
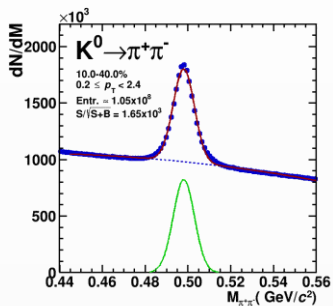
UrQMD, Bi+Bi,  $\sqrt{s_{NN}}=9.2$ , 10-40%, reconstructed (GEANT4) – production 25



- Reconstructed and generated  $v_1$  and  $v_2$  for identified hadrons are in good agreement for all methods

AuAu@11 GeV (UrQMD), 25 M events  $\rightarrow$  full event/detector simulation and reconstruction

$$v_2^{SB}(\mathbf{m}_{inv}, \mathbf{p}_T) = v_2^S(\mathbf{p}_T) \frac{N^S(\mathbf{m}_{inv}, \mathbf{p}_T)}{N^{SB}(\mathbf{m}_{inv}, \mathbf{p}_T)} + v_2^B(\mathbf{m}_{inv}, \mathbf{p}_T) \frac{N^B(\mathbf{m}_{inv}, \mathbf{p}_T)}{N^{SB}(\mathbf{m}_{inv}, \mathbf{p}_T)}$$



- ❖ Differential flow signal extraction using invariant mass fit method
- ❖ Reasonable agreement between reconstructed and generated  $v_n$  signals for  $K_S^0$  and  $\Lambda$
- ❖ Similar measurements for weakly decaying hyperons and short-lived resonances

MPD has capabilities to measure different flow harmonics for a wide variety of identified hadrons in pp, p-A and A-A collisions

# Multi-Purpose Detector (MPD) Collaboration



*MPD International Collaboration was established in 2018 to construct, commission and operate the detector*

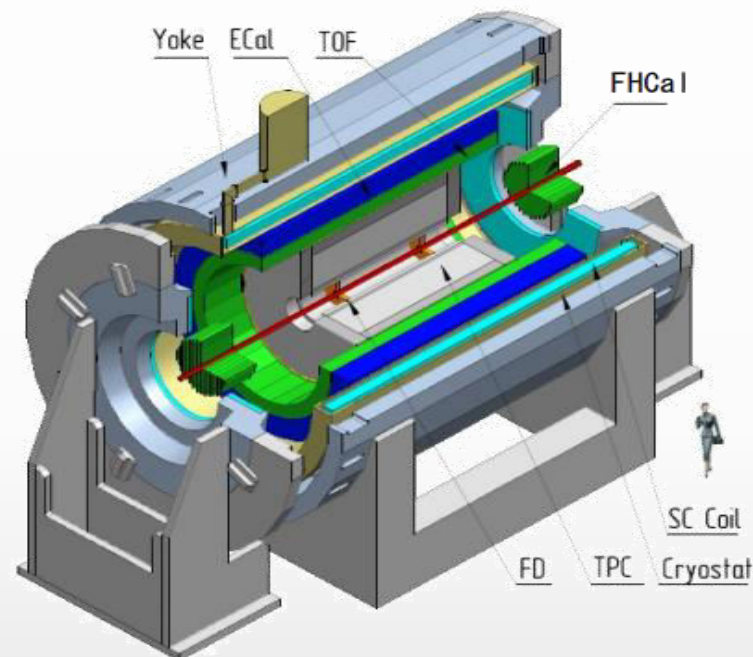
**11 Countries, >500 participants, 35 Institutes and JINR**

## Organization

**Acting Spokesperson:** **Victor Riabov**  
**Deputy Spokespersons:** **Zebo Tang, Arkadiy Taranenko**  
**Institutional Board Chair:** **Alejandro Ayala**  
**Project Manager:** **Slava Golovatyuk**

### **Joint Institute for Nuclear Research;**

A.Alikhanyan National Lab of Armenia, Yerevan, **Armenia**;  
University of Plovdiv, **Bulgaria**;  
Tsinghua University, Beijing, **China**;  
University of Science and Technology of China, Hefei, **China**;  
Huzhou University, Huzhou, **China**;  
Institute of Nuclear and Applied Physics, CAS, Shanghai, **China**;  
Central China Normal University, **China**;  
Shandong University, Shandong, **China**;  
University of Chinese Academy of Sciences, Beijing, **China**;  
University of South China, **China**;  
Three Gorges University, **China**;  
Institute of Modern Physics of CAS, Lanzhou, **China**;  
Tbilisi State University, Tbilisi, **Georgia**;  
Institute of Physics and Technology, Almaty, **Kazakhstan**;  
Benemérita Universidad Autónoma de Puebla, **Mexico**;  
Centro de Investigación y de Estudios Avanzados, **Mexico**;  
Instituto de Ciencias Nucleares, UNAM, **Mexico**;  
Universidad Autónoma de Sinaloa, **Mexico**;  
Universidad de Colima, **Mexico**;  
Universidad de Sonora, **Mexico**;  
Institute of Applied Physics, Chisinev, **Moldova**;  
Institute of Physics and Technology, **Mongolia**;



Belgorod National Research University, **Russia**;  
Institute for Nuclear Research of the RAS, Moscow, **Russia**;  
National Research Nuclear University MEPhI, Moscow, **Russia**;  
Moscow Institute of Science and Technology, **Russia**;  
North Osetian State University, **Russia**;  
National Research Center "Kurchatov Institute", **Russia**;  
Peter the Great St. Petersburg Polytechnic University Saint Petersburg, **Russia**;  
Plekhanov Russian University of Economics, Moscow, **Russia**;  
St.Petersburg State University, **Russia**;  
Skobeltsyn Institute of Nuclear Physics, Moscow, **Russia**;  
Petersburg Nuclear Physics Institute, Gatchina, **Russia**;  
Vinča Institute of Nuclear Sciences, **Serbia**;  
Pavol Jozef Šafárik University, Košice, **Slovakia**





- ❖ MPD construction and preparations for data taking are ongoing
- ❖ MPD commissioning and first data taking in 2025
- ❖ MPD has a solid physics program and can potentially provide unique results on the structure of the QCD phase diagram, provide insight into inner structure of compact star and neutron star mergers
- ❖ Develop realistic analysis techniques and tools using simulated data samples



# Annual workshops on physics performance studies at NICA

## Workshop on physics performance studies at NICA (NICA-2022)

13-15 December 2022

Virtual via ZOOM, Moscow time

Europe/Moscow timezone

Overview

Timetable

Participant List

Registration

↳ Registration Form

Group Photo

Previous workshops

Proceedings

### **3rd workshop on "Physics performance studies at FAIR and NICA"**

29 November-1 December 2021

<http://indico.oris.mephi.ru/event/221/>

### **2nd workshop on "Physics performance studies at FAIR and NICA"**

8-10 December 2020

<http://indico.oris.mephi.ru/event/209/>

### **1st workshop on "Physics performance studies at FAIR and NICA"**

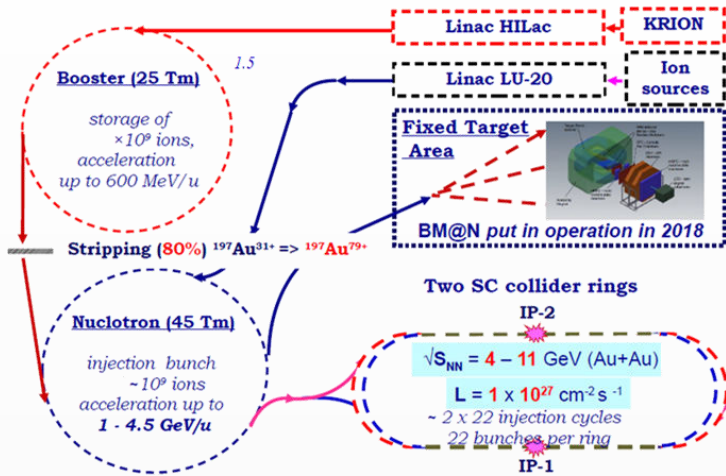
24-28 August 2020

<http://indico.oris.mephi.ru/event/181/>

Next workshop in December, 2023 – stay tuned for announcement

# BACKUP

# Milestones for accelerator complex



Booster



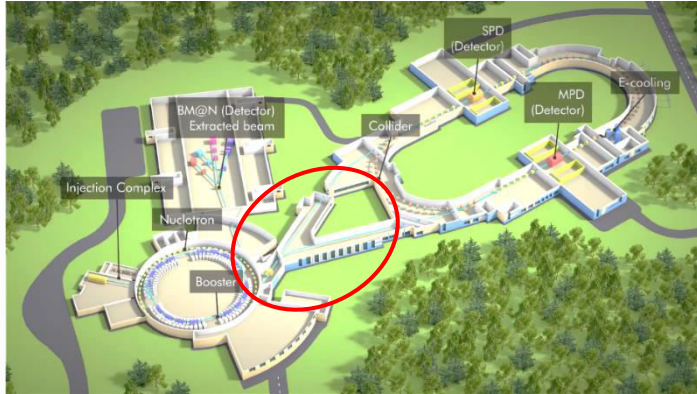
Nuclotron



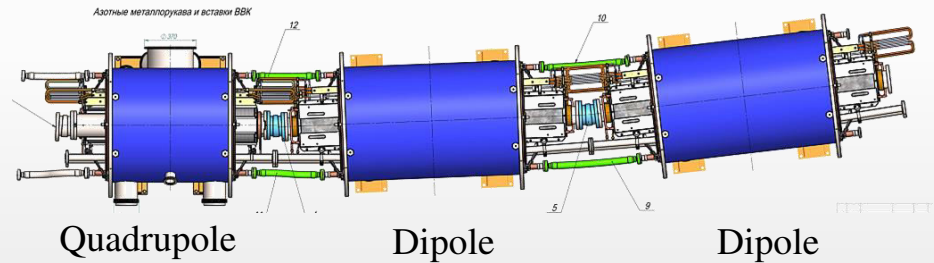
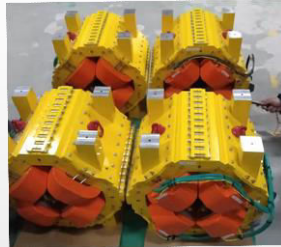
## ❖ Stages of the accelerator complex commissioning

- ✓ HILAC + transfer line to Booster  $\rightarrow$  commissioned in 2018 with  $\text{He}^{1+}$ ,  $\text{Fe}^{14+}$ ,  $\text{C}^{4+}$ ,  $\text{Ar}^{14+}$  and  $\text{Xe}^{28+}$
- ✓ HILAC + Booster  $\rightarrow$  first run in November-December, 2020 with  $\text{He}^{1+}$
- ✓ HILAC + Booster + transfer line to Nuclotron  $\rightarrow$  second run in October, 2021 with  $\text{He}^{1+}$  and  $\text{Fe}^{16+}$
- ✓ HILAC + Booster + Nuclotron + transfer line to BM@N  $\rightarrow$  third run in Jan. – Apr., 2022 with  $\text{C}^{6+}$
- ✓ HILAC + Booster + Nuclotron + transfer line to BM@N  $\rightarrow$  fourth run in September, 2022 – February, 2023 with Ar and Xe beams  $\rightarrow$  500+ M events at BM@N

Nuclotron-NICA transfer line

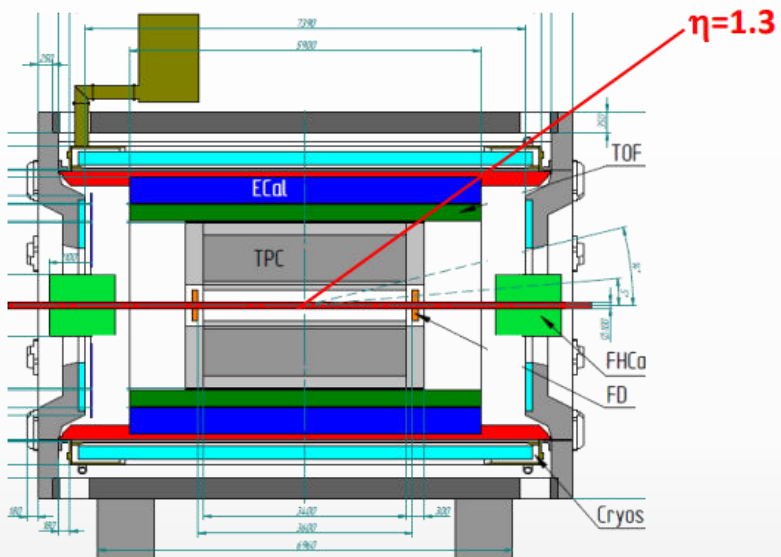


NICA collider



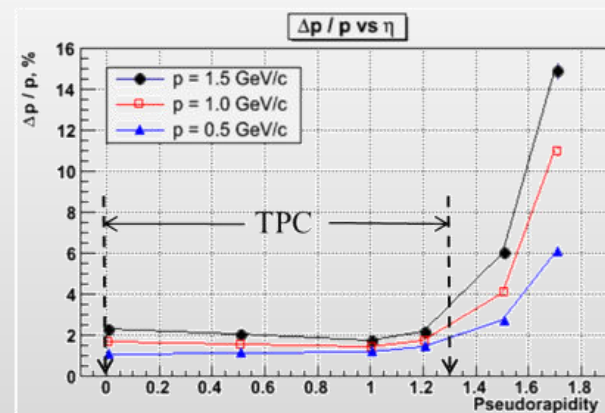
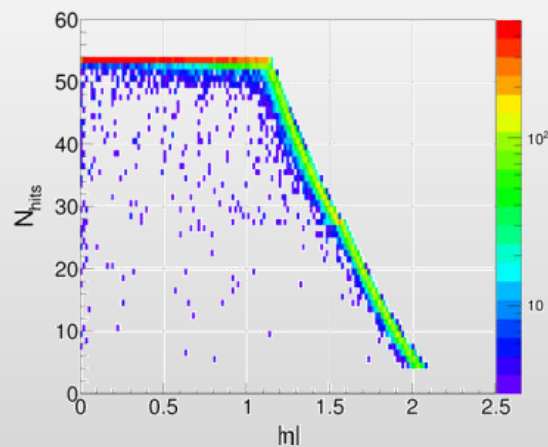
- ❖ Magnet and RF installation: by the middle of 2024
- ❖ First technological and cryogenic run of collider: end of 2024 - beginning of 2025
- ❖ Fast extraction system from the Nuclotron: June of 2024
- ❖ Nuclotron-collider transfer line: Autumn of 2024
- ❖ First run with beams: 2025

## MPD setup and overall performance



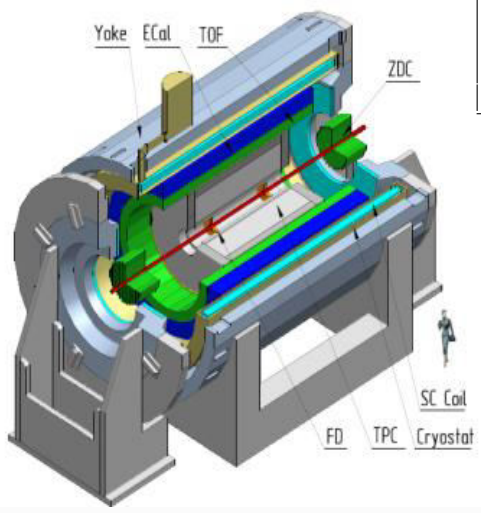
### MPD at Stage'1:

- *TPC tracking*:  $|\eta| < 1.6$  ( $N_{\text{points}} > 15$ )
- *TOF & ECal coverage*:  $|\eta| < 1.3$
- *PID*: TOF+dE/dx combined  $|\eta| < 1.3$ ,  $pT < 3$  GeV/c, limited PID  $1.3 < |\eta| < 1.6$  (dE/dx)



# Multi-Purpose Detector

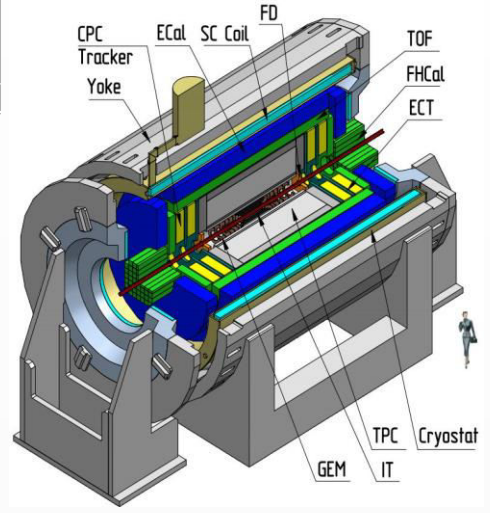
## Stage- I



Length	340 cm
Vessel outer radius	140 cm
Vessel inner radius	27 cm
Default magnetic field	0.5 T
Drift gas mixture	90% Ar+10% CH <sub>4</sub>
Maximum event rate	7 kHz ( $L = 10^{27} \text{ cm}^{-2} \text{ s}^{-1}$ )



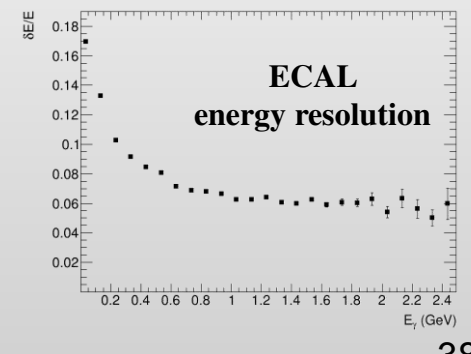
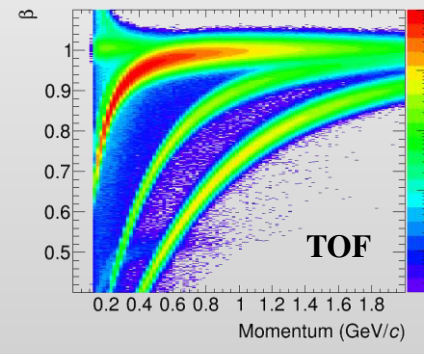
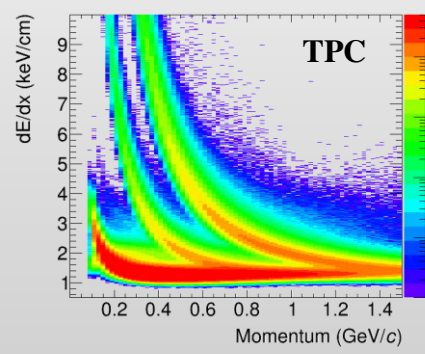
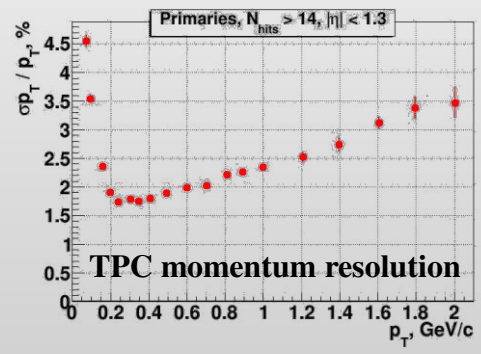
## Stage- II



- TPC:**  $|\Delta\phi| < 2\pi, |\eta| \leq 1.6$
- TOF, EMC:**  $|\Delta\phi| < 2\pi, |\eta| \leq 1.4$
- FFD:**  $|\Delta\phi| < 2\pi, 2.9 < |\eta| < 3.3$
- FHCAL:**  $|\Delta\phi| < 2\pi, 2 < |\eta| < 5$

- + ITS** (heavy-flavor measurements)
- + forward spectrometers**

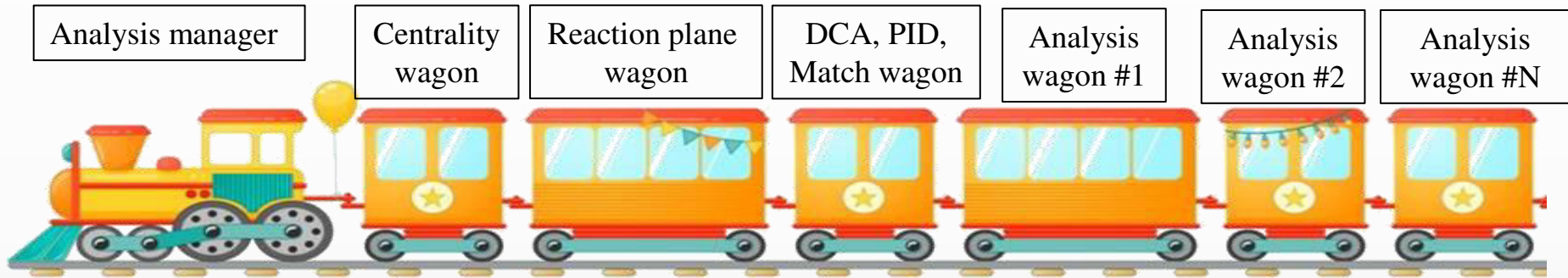
Au+Au @ 11 GeV (UrQMD + full chain reconstruction)



- ❖ Physics feasibility studies using centralized large-scale MC productions → consistent picture of the MPD physics capabilities with the first data sets, preparation for real data analyses
- ❖ <https://mpdforum.jinr.ru/c/mcprod/26>:
  - Request 25: General-purpose, 50M UrQMD BiBi@9.2 → **DONE**
  - Request 26: General-purpose (trigger), 1M DCM-QGSM-SMM BiBi@9.2 → **DONE**
  - Request 27: General-purpose (trigger), 1M PHQMD BiBi@9.2 → **DONE**
  - Request 28: General-purpose with reduced magnetic field, 10M UrQMD BiBi@9.2 → **DONE**
  - Request 29: General-purpose (hypernuclei), 20M PHQMD BiBi@9.2 → **DONE**
  - Request 30: General-purpose (polarization), 15M PHSD BiBi@9.2 → **DONE**
  - Request 31: General-purpose (femtoscapy), 50 M UrQMD BiBi@9.2 with freeze-out → **Running**
  - Request 32: General purpose (flow), 15M vHLLE+UrQMD with XPT → **DONE**
  - Request 33: General purpose (FXT), (11M x 3 energies) UrQMD (mean field) → **DONE**
- ❖ Production comparable in size to the first expected real data samples test the existing computing and software infrastructure
- ❖ Develop realistic analysis methods and techniques, set priorities and find group leaders

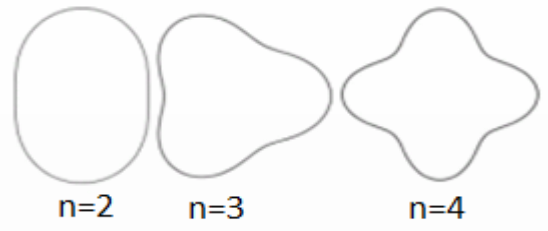
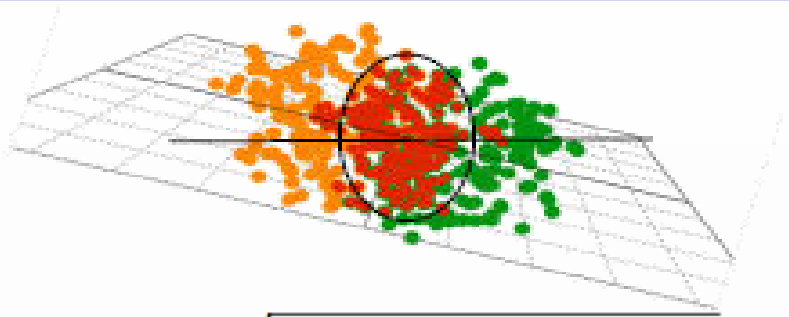
# Handling the big data sets

- ❖ Centralized Analysis Framework for access and analysis of data → Analysis Train:
  - ✓ consistent approaches and results across collaboration, easier storage and sharing of codes and methods
  - ✓ reduced number of input/output operations for disks and databases, easier data storage on tapes
- ❖ Analysis manager reads event into memory and calls wagons one-by-one to modify and/or analyze data:



- ❖ The Analysis manager and the first Wagons have been created, in MpdRoot @ mpdroot/physics
- ❖ Eventually all analysis codes will be committed to MpdRoot as Wagons
- ❖ The Train runs to process centralized mass productions
  - 50M events are processed in 7-8 hours with ~ 15 wagons (1 year of CPU time)





$$\epsilon_n = \sqrt{\frac{\langle r^n \cos n\phi \rangle + \langle r^n \sin n\phi \rangle}{\langle r^n \rangle}}$$

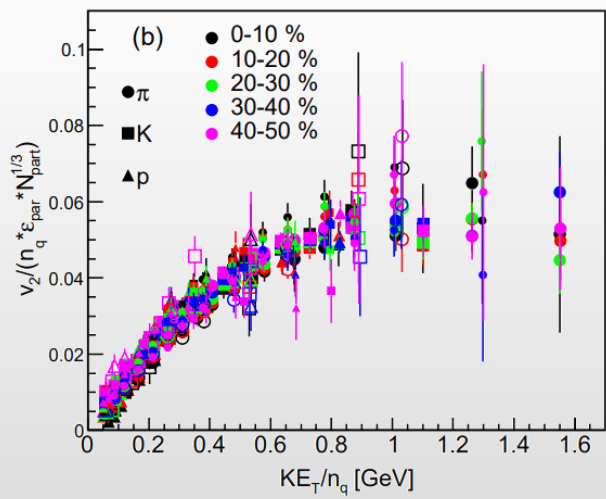
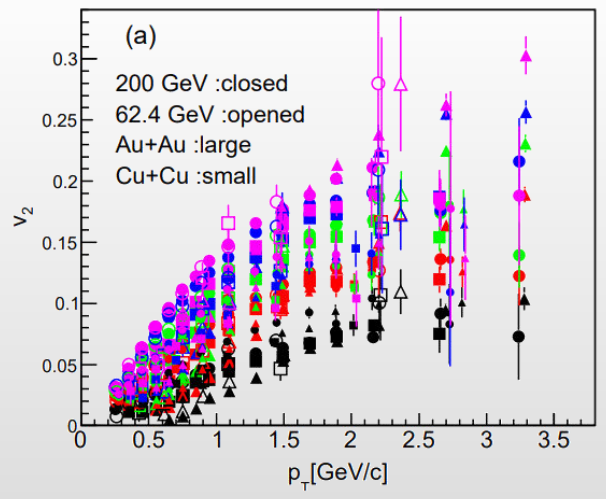
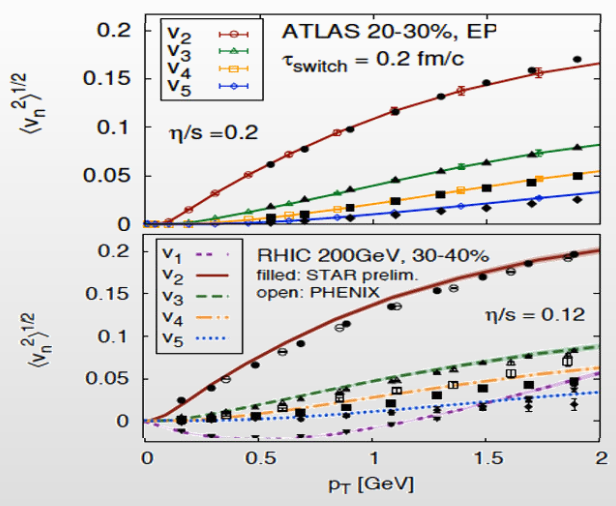


$$\frac{dN}{d\phi} \propto \left( 1 + 2 \sum_{n=1} v_n \cos [n(\phi - \Psi_n)] \right)$$

❖ Initial eccentricity and its fluctuations drive momentum anisotropy  $v_n$  with specific viscous modulation

Gale, Jeon et al., Phys. Rev. Lett. 110, 012302

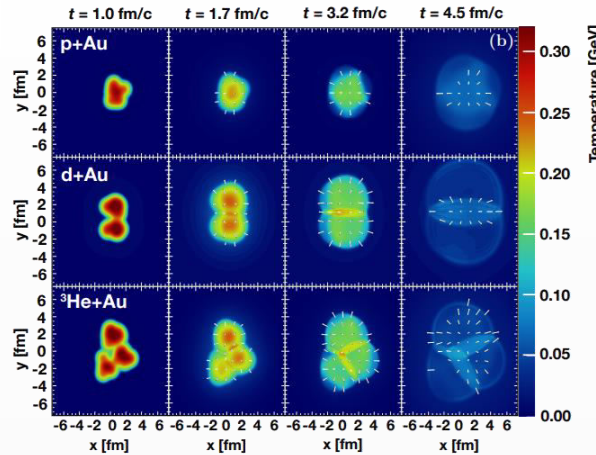
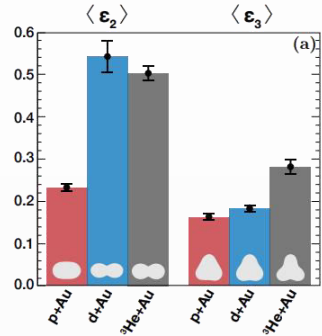
Phys.Rev.C 92 (2015) 3, 034913



- ❖ Evidence for a dense perfect liquid found at RHIC/LHC (*M. Roizard et al., Scientific American, 2006*)
- ❖ System size scan (A-A) is an important part of systematic study (initial geometry  $\rightarrow$  flow harmonics)

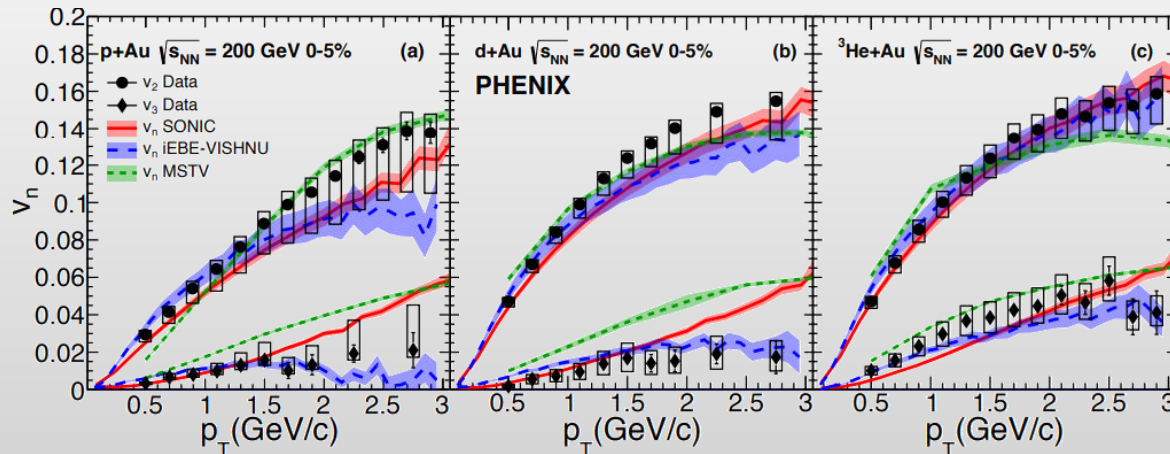
*Nature Phys.* 15 (2019) 3, 214-220

$$\epsilon_n = \frac{\sqrt{\langle r^n \cos(n\phi) \rangle^2 + \langle r^n \sin(n\phi) \rangle^2}}{\langle r^n \rangle}$$



p-Au, d-Au and  $^3\text{He}$ -Au @ 200 GeV by PHENIX

- ❖ Measurements demonstrate that the  $v_n$ 's are correlated to the initial geometry
- ❖ Hydrodynamical models, which include the formation of short-lived QGP droplets, provide a simultaneous description of these measurements



# Event plane Resolution

in vHLE+UrQMD Bi+Bi  $\sqrt{s_{NN}} = 9.2$  GeV

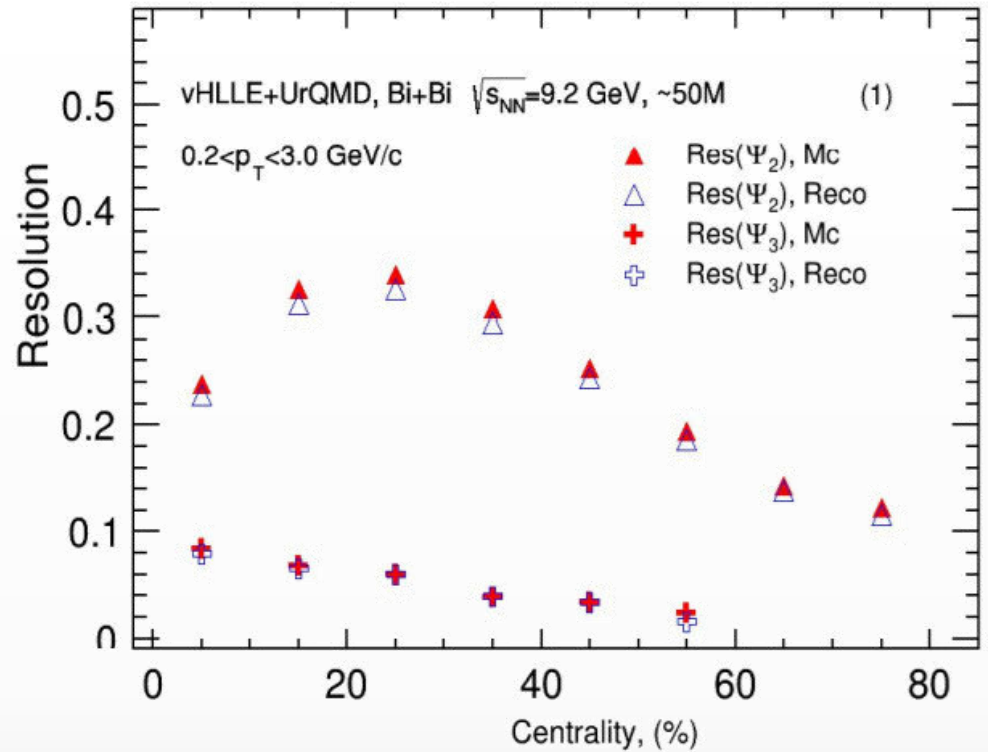
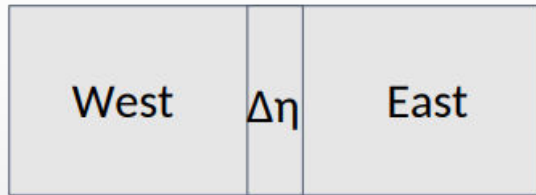
2 sub event:  $\Delta\eta=0.1$

$$Res\{\Psi_n^{E(W)}\} = \sqrt{\langle \cos [n(\Psi_n^E - \Psi_n^W)] \rangle}$$

Anisotropic flow is measured as follows:

$$v_n = \frac{\langle \cos [n(\phi - \Psi_n^{EP})] \rangle}{\sqrt{\langle \cos [n(\Psi_{n,a} - \Psi_{n,b})] \rangle}}$$

TPC



Mass [production 32](#) was used

- We do not measure the  $\Psi_3$  resolution after to 60% centrality
- $\Psi_3$  resolution are smaller than  $\Psi_2$
- Good agreement between  $R_{MC}(\Psi_n)$  and  $R_{reco}(\Psi_n)$

13

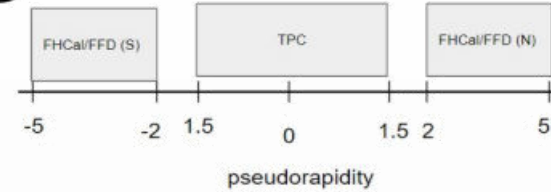
# FHCal and FFD comparison for $v_n$ in MPD

true

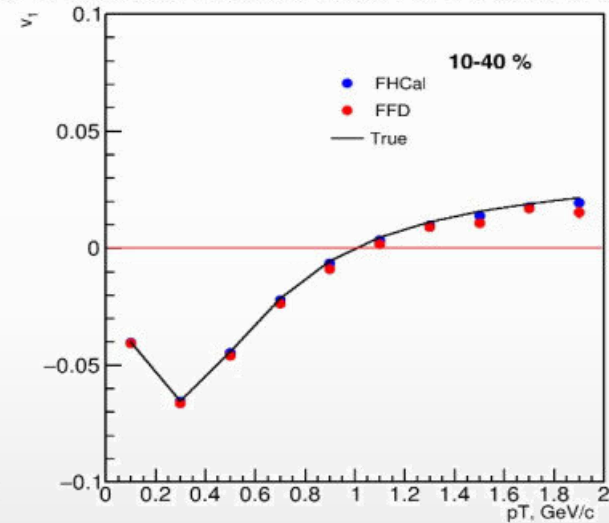
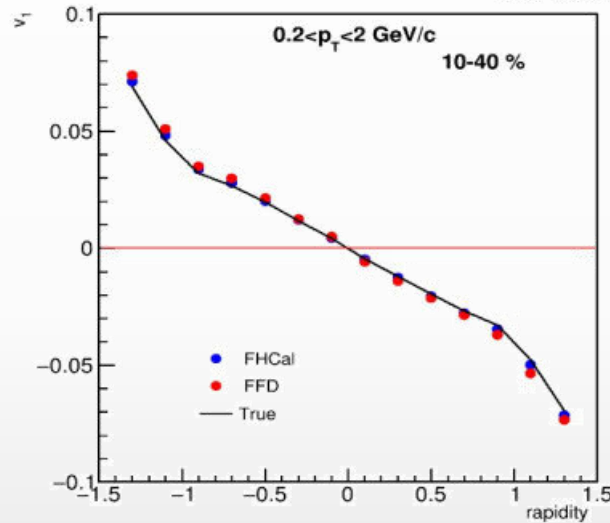
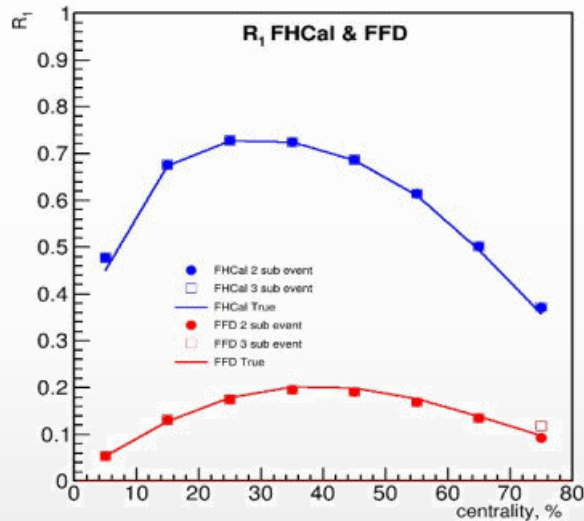
2 sub events

3 sub events

$$R_{1,i}^{True} = \langle Q_{1,i} \Psi_{RP} \rangle \quad R_{1,i} = \sqrt{\langle Q_{1,i}^N Q_{1,i}^S \rangle}, i = x, y \quad R_{1,i}^N = \sqrt{\frac{2\langle Q_{1,i}^N Q_{1,i}^S \rangle \langle Q_{1,i}^S Q_{1,i}^{TPC} \rangle}{\langle Q_{1,i}^N Q_{1,i}^{TPC} \rangle}}$$



See details in V.Troshin's talk on Cross-PWG 14.02.2023



Resolution from FFD is considerably smaller than from FHCal  
Flow results using FFD and FHCal are consistent

# Elliptic flow measurements using TPC: Scalar product, Event-plane

$$u_2 = \cos 2\phi + i \sin 2\phi = e^{2i\phi}$$

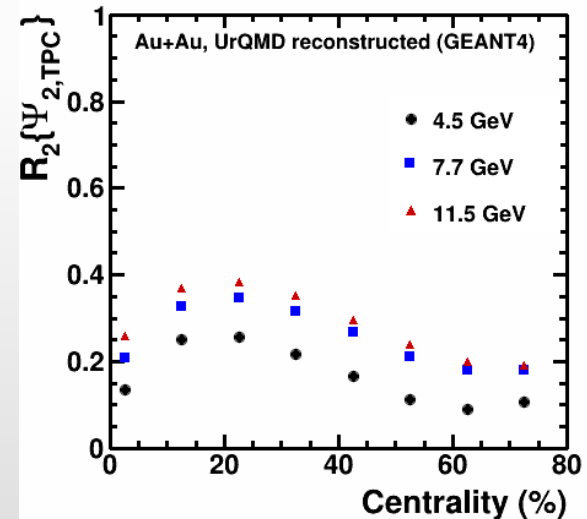
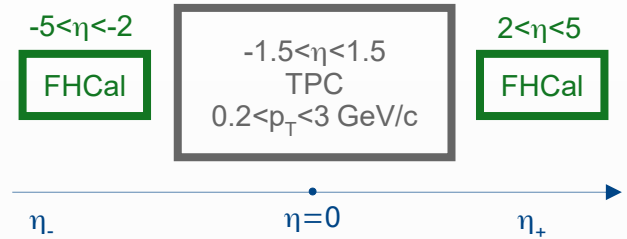
$$Q_2 = \sum_{j=1}^M \omega_j u_{2,j}, \quad \Psi_{2,\text{TPC}} = \frac{1}{2} \tan^{-1} \left( \frac{Q_{2,y}}{Q_{2,x}} \right)$$

- **Scalar product:** 
$$v_2^{\text{SP}} \{Q_{2,\text{TPC}}\} = \frac{\langle u_{2,\eta\pm} Q_{2,\eta\mp}^* \rangle}{\sqrt{\langle Q_{2,\eta+} Q_{2,\eta-} \rangle}}$$

- **TPC Event-plane:**

$$v_2^{\text{EP}} \{\Psi_{2,\text{TPC}}\} = \frac{\langle \cos [2(\phi_{\eta\pm} - \Psi_{2,\eta\mp})] \rangle}{R_2^{\text{EP}} \{\Psi_{2,\text{TPC}}\}}$$

$$R_2^{\text{EP}} \{\Psi_{2,\text{TPC}}\} = \sqrt{\langle \cos [2(\Psi_{2,\eta+} - \Psi_{2,\eta-})] \rangle}$$



- ❖ Data taking by STAR at RHIC:  $3 < \sqrt{s_{NN}} < 200$  GeV ( $750 < \mu_B < 25$  MeV)

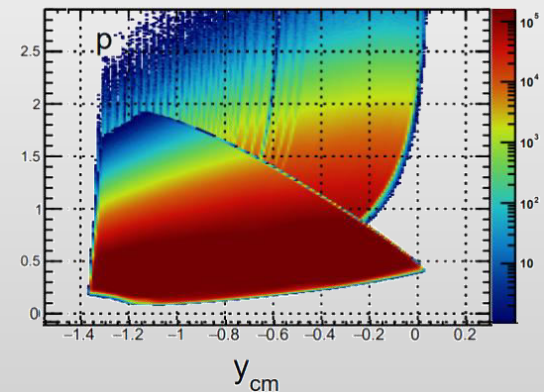
Au+Au Collisions at RHIC											
Collider Runs						Fixed-Target Runs					
	$\sqrt{s_{NN}}$ (GeV)	#Events	$\mu_B$	$y_{beam}$	run		$\sqrt{s_{NN}}$ (GeV)	#Events	$\mu_B$	$y_{beam}$	run
1	200	380 M	25 MeV	5.3	Run-10, 19	1	13.7 (100)	50 M	280 MeV	-2.69	Run-21
2	62.4	46 M	75 MeV		Run-10	2	11.5 (70)	50 M	320 MeV	-2.51	Run-21
3	54.4	1200 M	85 MeV		Run-17	3	9.2 (44.5)	50 M	370 MeV	-2.28	Run-21
4	39	86 M	112 MeV		Run-10	4	7.7 (31.2)	260 M	420 MeV	-2.1	Run-18, 19, 20
5	27	585 M	156 MeV	3.36	Run-11, 18	5	7.2 (26.5)	470 M	440 MeV	-2.02	Run-18, 20
6	19.6	595 M	206 MeV	3.1	Run-11, 19	6	6.2 (19.5)	120 M	490 MeV	1.87	Run-20
7	17.3	256 M	230 MeV		Run-21	7	5.2 (13.5)	100 M	540 MeV	-1.68	Run-20
8	14.6	340 M	262 MeV		Run-14, 19	8	4.5 (9.8)	110 M	590 MeV	-1.52	Run-20
9	11.5	157 M	316 MeV		Run-10, 20	9	3.9 (7.3)	120 M	633 MeV	-1.37	Run-20
10	9.2	160 M	372 MeV		Run-10, 20	10	3.5 (5.75)	120 M	670 MeV	-1.2	Run-20
11	7.7	104 M	420 MeV		Run-21	11	3.2 (4.59)	200 M	699 MeV	-1.13	Run-19
						12	3.0 (3.85)	2000 M	750 MeV	-1.05	Run-18, 21

- ❖ A very impressive and successful program with many collected datasets, already available and expected results

- ❖ Limitations:

- ✓ Au+Au collisions only
- ✓ Among the fixed-target runs, only the 3 GeV data have full mid-rapidity coverage for protons ( $|y| < 0.5$ ), which is crucial for physics observables

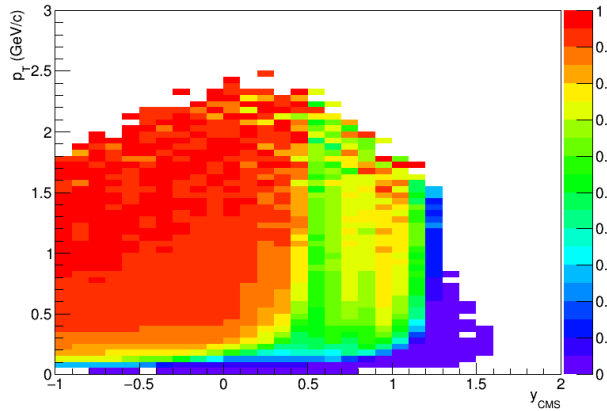
Au+Au @ 3.9 GeV



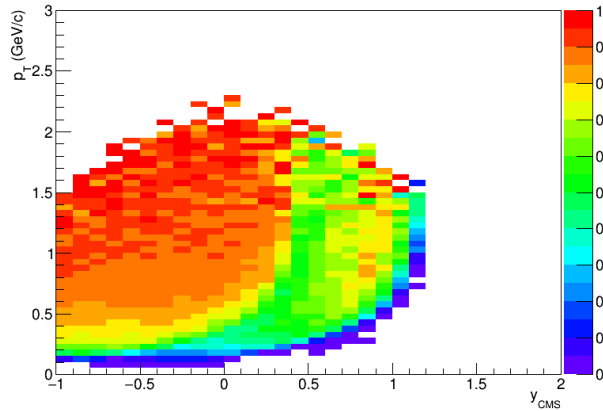
# Efficiency for $\pi/K/p$ , $E_{\text{lab}} = 5.5 \cdot A \text{ GeV}$

- $N_{\text{hits}} > 10$ ;  $DCA < 2 \text{ cm}$ ; Primary particles ( $R_{\text{production}} < 1 \text{ cm}$ )

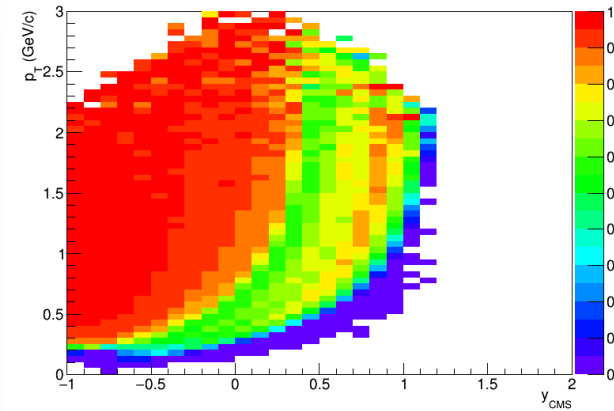
$\pi^\pm$ , TPC



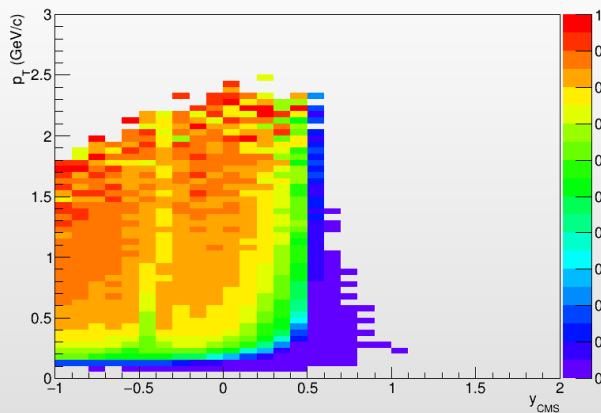
$K^\pm$ , TPC



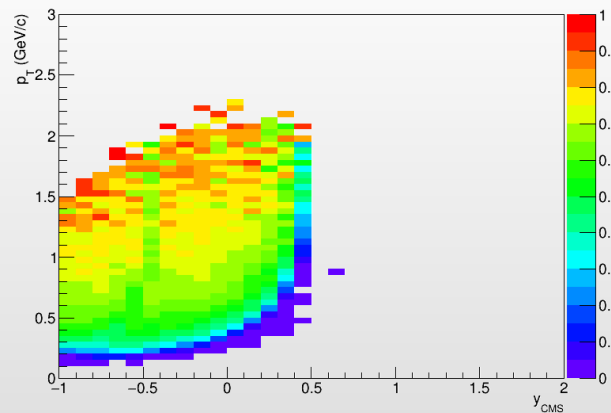
p and  $\bar{p}$ , TPC



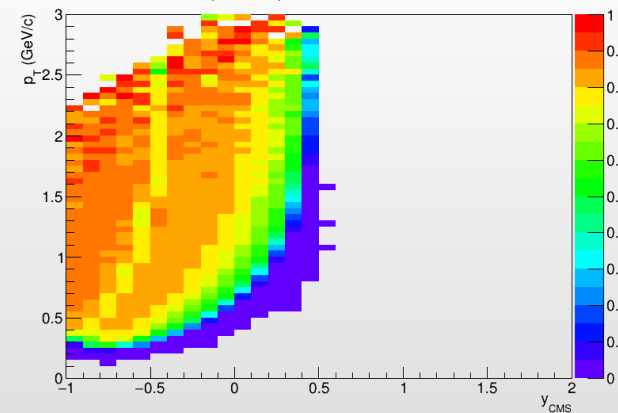
$\pi^\pm$ , TPC & TOF



$K^\pm$ , TPC & TOF

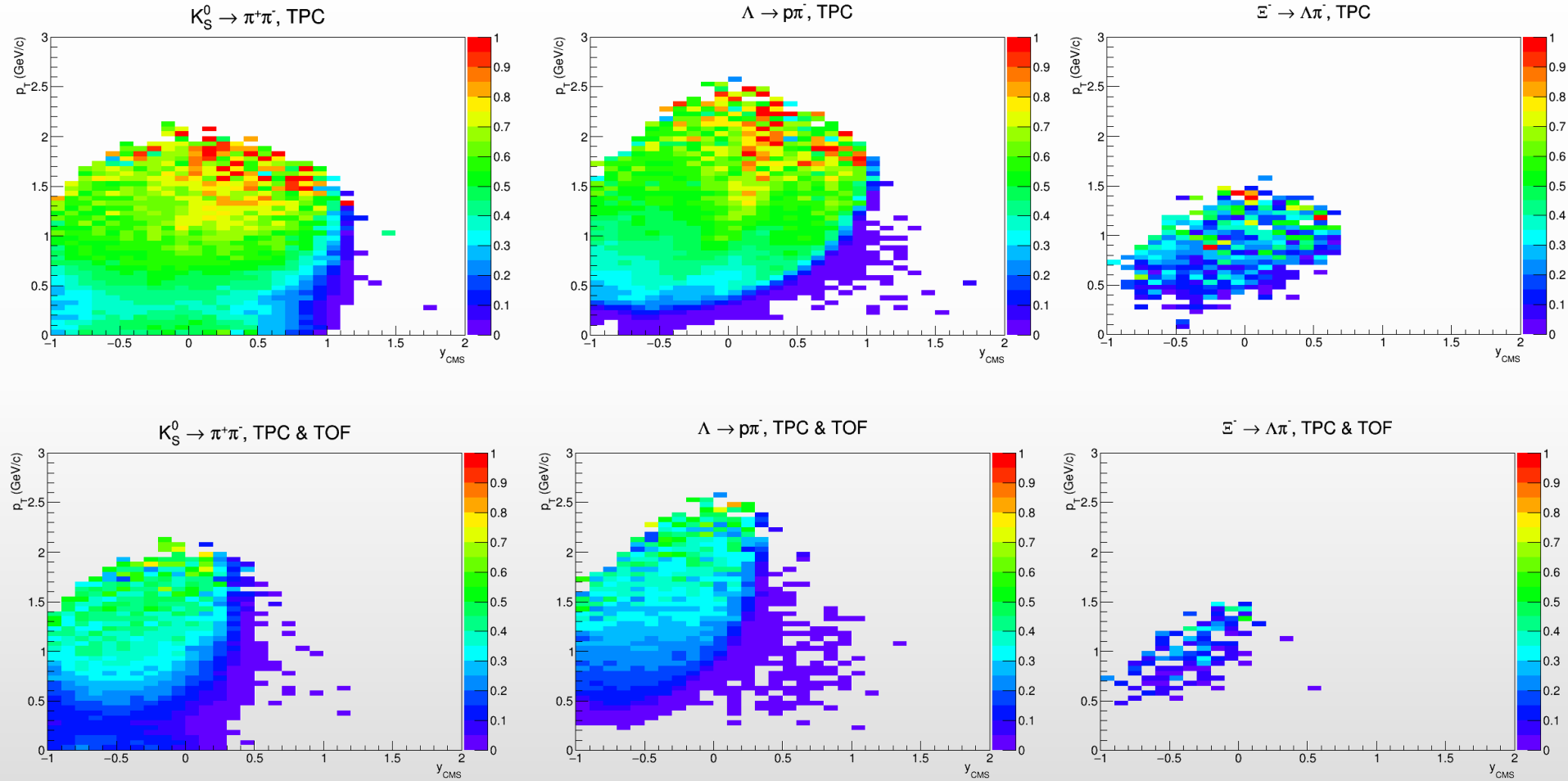


p and  $\bar{p}$ , TPC & TOF



# Efficiency for $K_S^0/\Lambda/\Xi^-$ , $E_{\text{lab}} = 5.5 \cdot A \text{ GeV}$

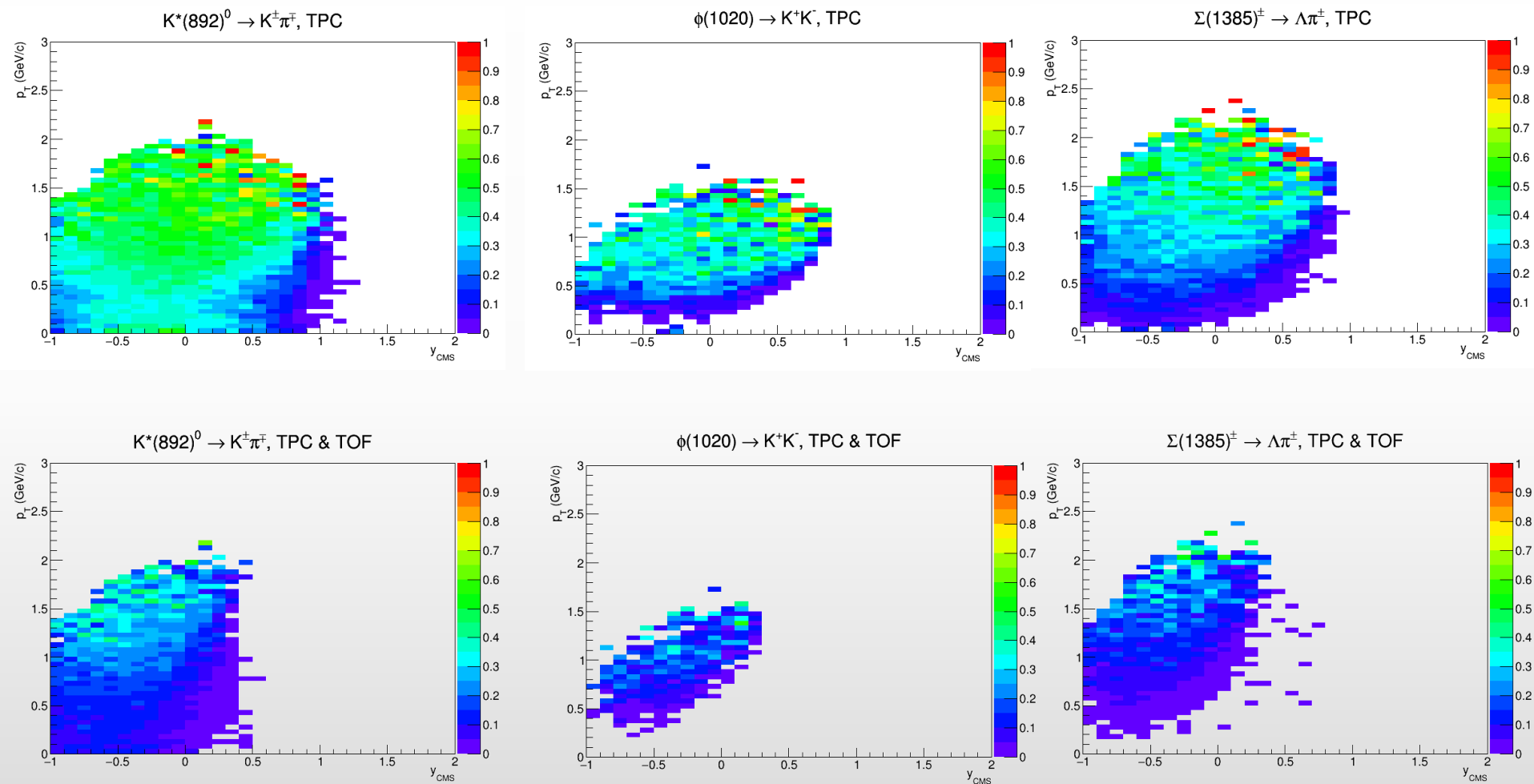
- $N_{\text{hits}} > 10$ ;  $p_T > 0.1 \text{ GeV}/c$ ; Primary particles ( $R_{\text{production}} < 1 \text{ cm}$ )





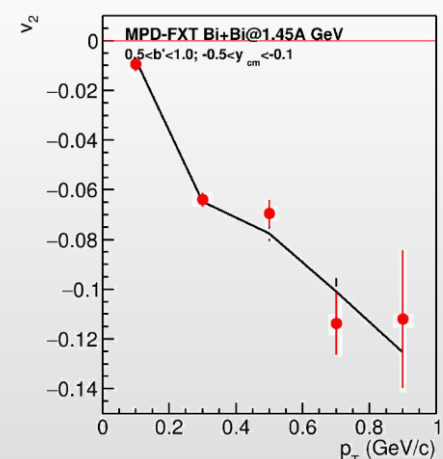
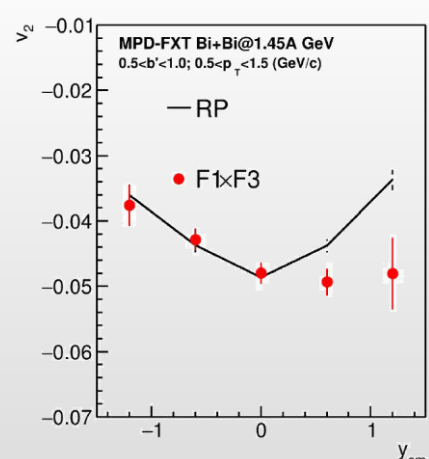
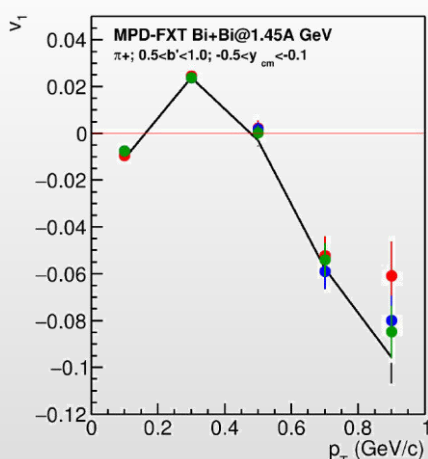
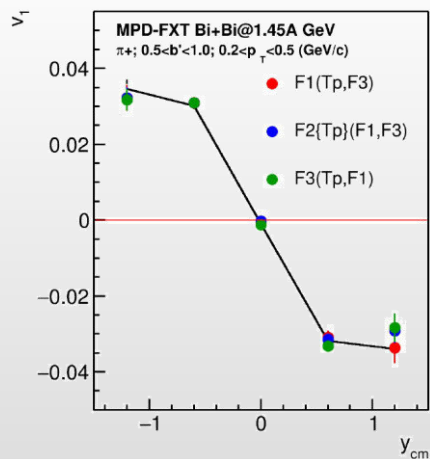
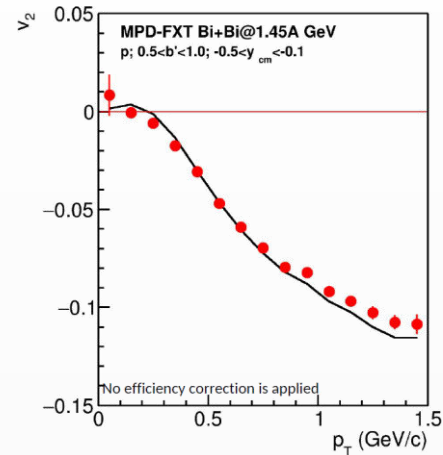
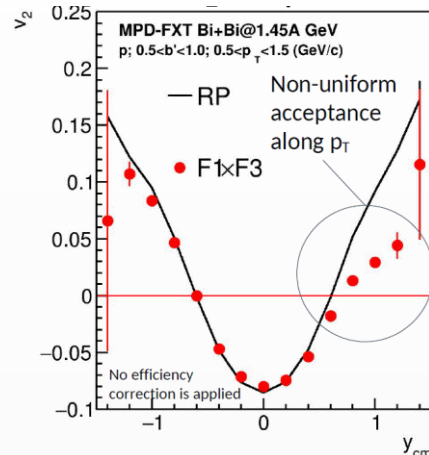
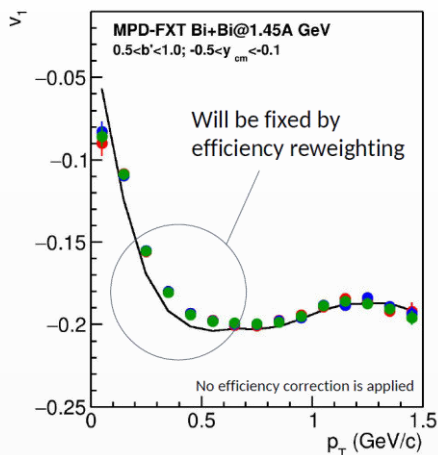
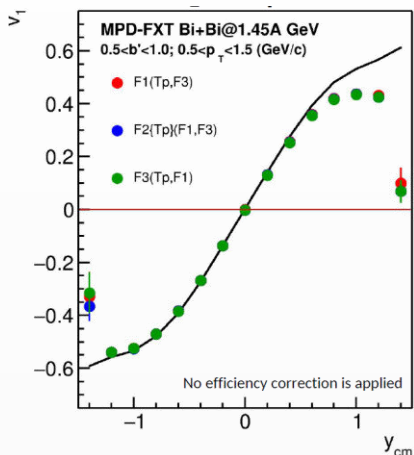
# Efficiency for $K^*(892)^0/\phi(1020)/\Sigma(1385)^\pm$ , $E_{\text{lab}} = 5.5\text{-A GeV}$

- $N_{\text{hits}} > 10$ ;  $p_T > 0.1 \text{ GeV}/c$ ; Primary particles ( $R_{\text{production}} < 1 \text{ cm}$ )



MPD should be able light and heavy identified hadrons at midrapidity

❖ Request 33 mass production (UrQMD mean-field, fixed-target mode)

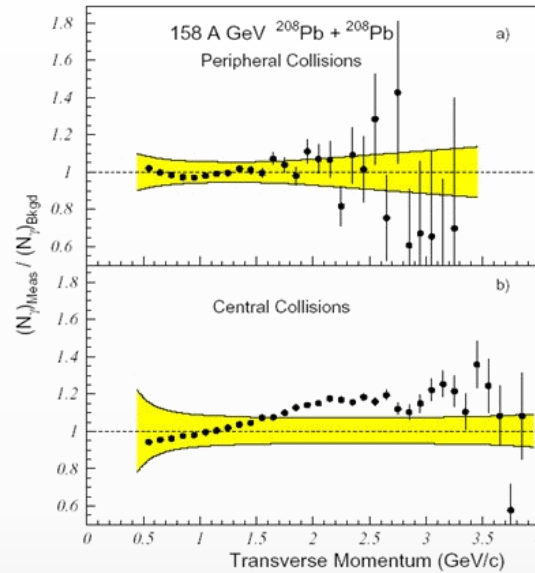
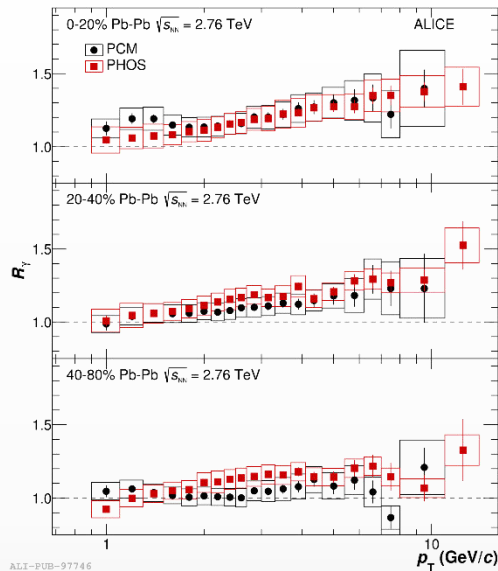


Reconstructed  $v_1$  &  $v_2$  are qualitatively consistent with truly generated signals at  $|y_{cms}| < 0.5$

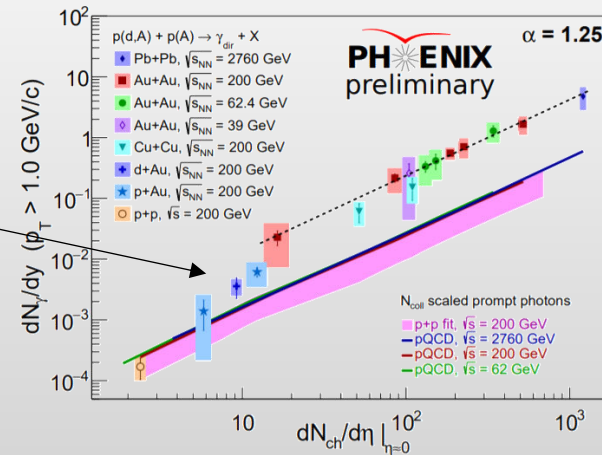
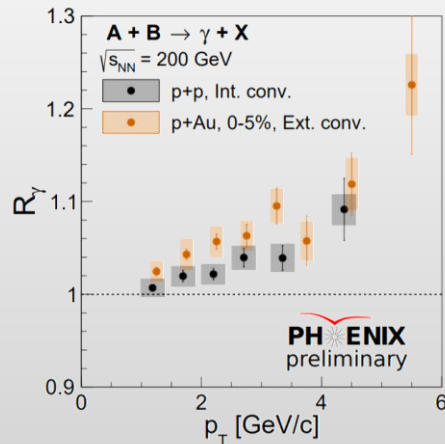
Efficiency corrections and larger statistics are needed for numerical conclusions

# Comparison to higher energies

- $R_\gamma \sim 1.05-1.2$  in heavy-ion collisions at SPS/RHIC/LHC,  $\sqrt{s_{NN}} = 17.2-2760$  GeV



- $R_\gamma \sim 1.05$  is on the verge of experimental measurability (PHENIX in pp/pA@200,  $\geq 2\sigma$ )



# Finite-Size Effects and search for CEP

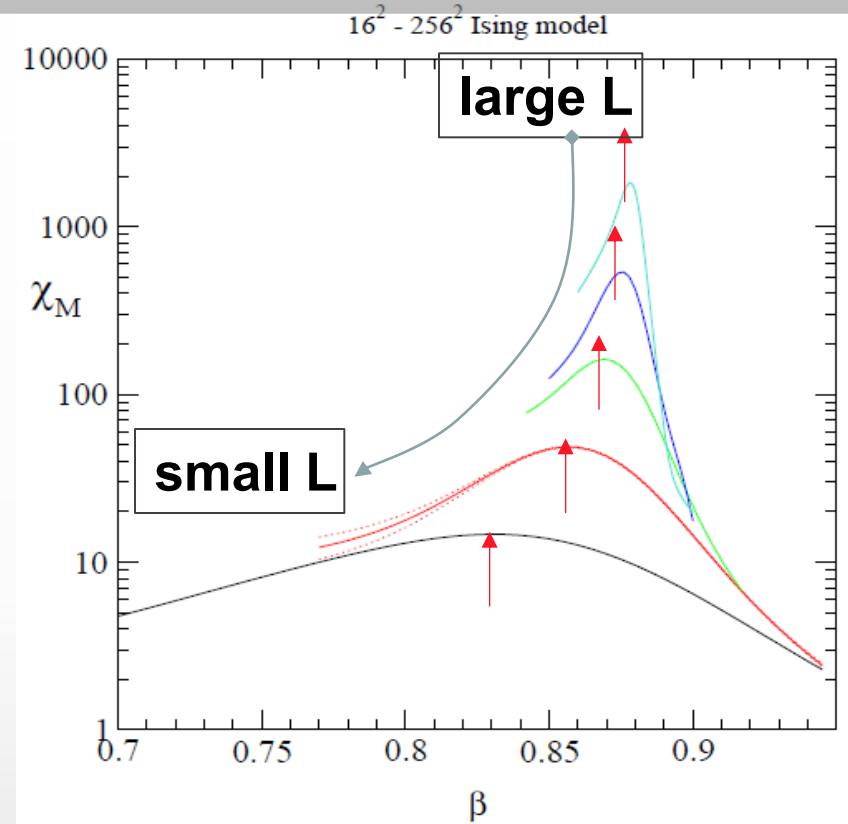
In HIC, both the size ( $L$ ) and duration of formed system are finite.

## Critical behavior changes with $L$

If the  $L$  is too small, the correlation length  $\xi$  can not be fully developed to cause a phase transition.

if the correlation length  $\xi \sim |T - T_c|^{-\nu} \leq L$  the finite-size effect is not negligible and only a **pseudo-critical point, shifted from the genuine CEP, is observed.**

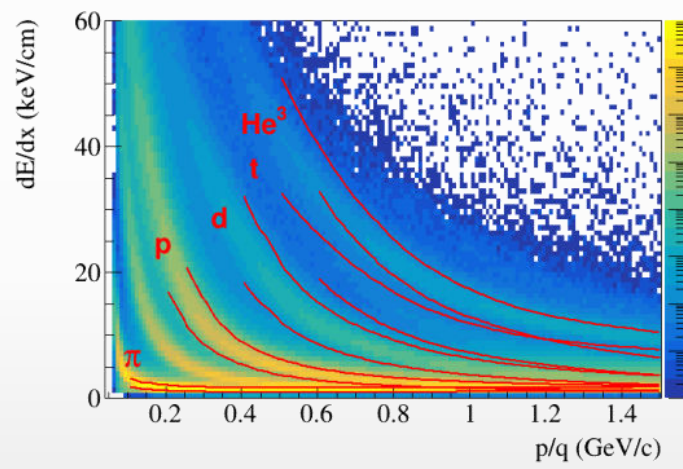
- ✓ Finite-size effects have a specific dependencies on size ( $L$ )
- ✓ The scaling of these dependencies give access to the CEP's location, it's critical exponents and scaling function.



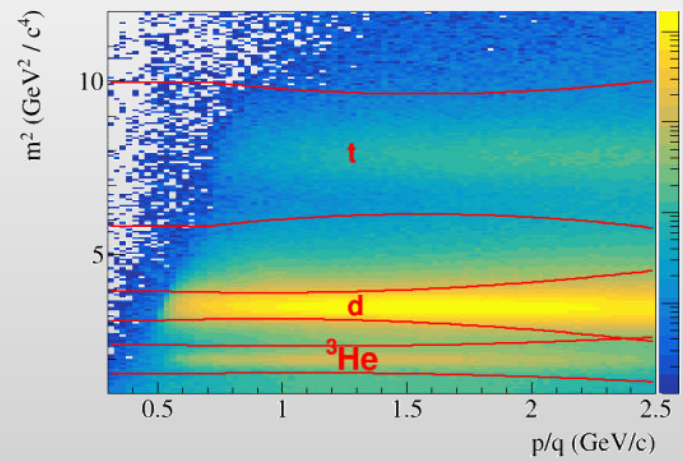
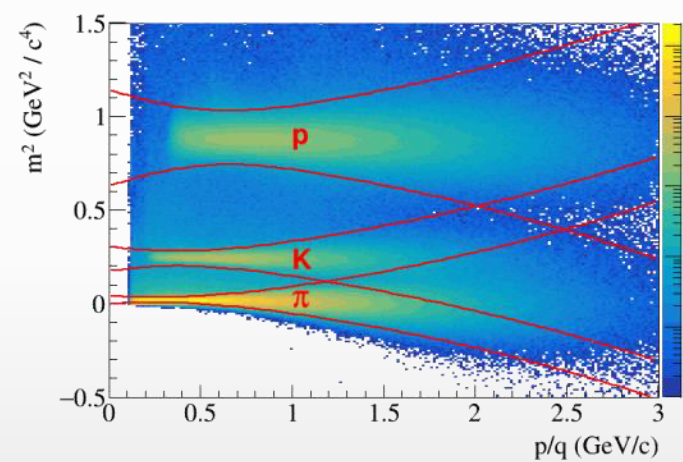
Note change in peak heights positions & widths with  $L$

- ❖ NICA can deliver different ion beam species and energies:
  - ✓ Targets of interest (C = astronaut, Si = electronics, Al = spacecraft) + He, C, O, Si, Fe, etc.
- ❖ No data exist for projectile energies > 3 GeV/n

dE/dx vs momentum in TPC



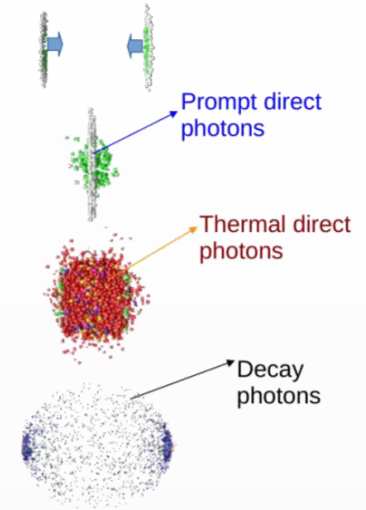
$m^2$  vs. momentum in TOF



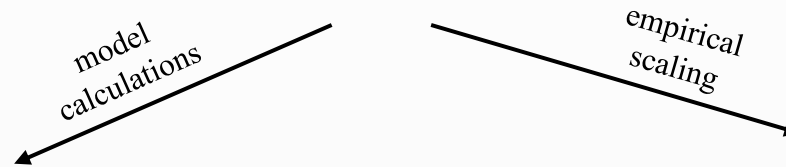
MPD has excellent light fragment identification capabilities in a wide rapidity range → unique capability of the MPD in the NICA energy range

# Direct photons

- ❖ Direct photons – photons not from hadronic decays.
- ❖ Produced throughout the system evolution (thermal + prompt) :
  - ✓ penetrating probe
  - ✓ low-E - most direct estimation of the effective system temperature
  - ✓ high-E - hard scattering probe



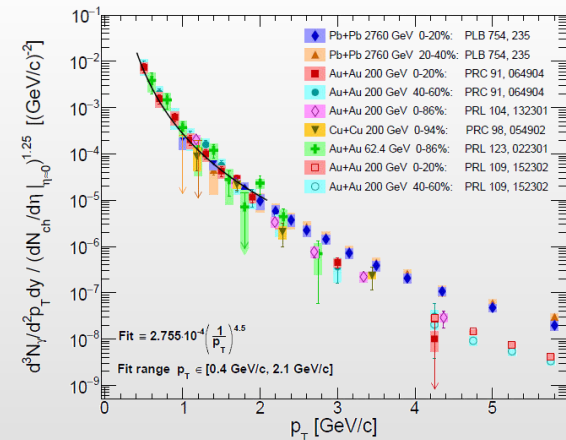
## Estimation of the direct photon yields @NICA



*Physics of Particles and Nuclei, 2021, Vol. 52, No. 4, pp. 681–685*

- ✓ UrQMD v3.4 with hybrid model (3+1D hydro, bag model EoS, hadronic rescattering and resonances within UrQMD)
- ✓ each cell have  $T_i, E_i, \mu_{bi}$ :
  - $T$  is high – QGP phase (Peter Arnold, Guy D. Moore, Laurence G. Yaffe, JHEP 0112:009 2001)
  - $T$  is low – HG phase (Simon Turbide, Ralf Rapp, Charles Gale, Phys.Rev.C69:014903,2004)
  - $T$  is intermediate – mixed phase
- ✓ integrate over all cells and all time steps
- ✓ calculations reproduce hydro calculations for the SPS

*Phys.Rev.Lett. 123 (2019) 2, 022301*



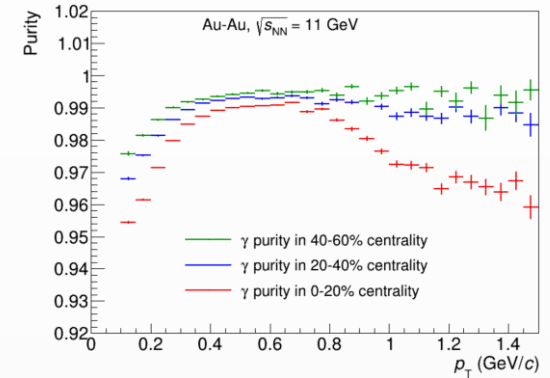
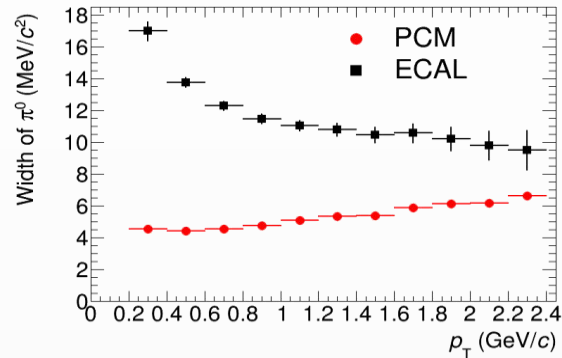
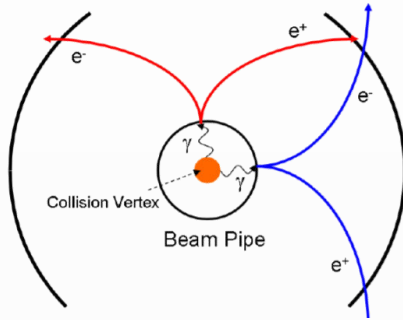
$$R_\gamma = \frac{\gamma_{\text{inc}}}{\gamma_{\text{decay}}} = \frac{\gamma_{\text{inc}}/\pi^0}{\gamma_{\text{decay}}/\pi^0_{\text{param}}} \quad \gamma_{\text{direct}} = \left(1 - \frac{1}{R_\gamma}\right) \cdot \gamma_{\text{inc}}$$

- ❖ Non-zero direct photon yields are predicted with  $R_\gamma \sim 1.05 - 1.15$  and  $v_2 \sim 0.5\%$  at top NICA energy

# Prospects for the MPD

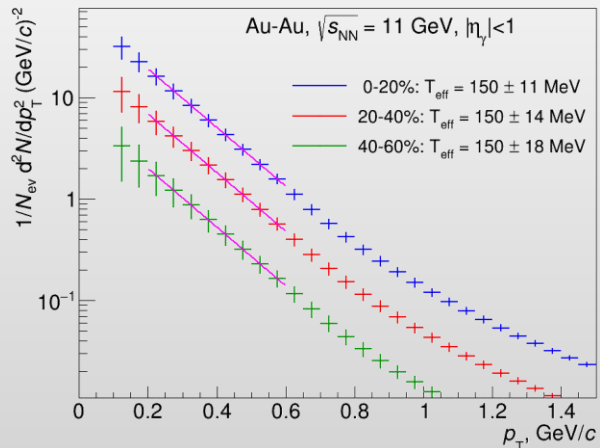
- ❖ Photons can be measured in the ECAL or in the tracking system as  $e^+e^-$  conversion pairs (PCM)

beam pipe (0.3%  $X_0$ ) + inner TPC vessels (2.4%  $X_0$ )



- ❖ Main sources of systematic uncertainties for direct photons:

- ✓ detector material budget  $\rightarrow$  conversion probability
- ✓  $\pi^0$  reconstruction efficiency
- ✓  $p_T$ -shapes of  $\pi^0$  and  $\eta$  production spectra



- ✓ ECAL and PCM for photon reconstruction and measurement of neutral mesons (background)
- ✓ With  $R_\gamma \sim 1.1$  and  $\delta R_\gamma/R_\gamma \sim 3\%$   $\rightarrow$  uncertainty of  $T_{\text{eff}} \sim 10\%$
- ✓ Development of reconstruction techniques and estimation of needed statistics are in progress

$\rightarrow$  potentially, MPD can provide unique measurements for direct photon production in the NICA energy range